J|A|C|S
ARTICLES
Published on Web 01/10/2004

The Photochemistry of Polydonor-Substituted Phthalimides: Curtin-Hammett-Type Control of Competing Reactions of Potentially Interconverting Zwitterionic Biradical Intermediates

Ung Chan Yoon,*[,†] Hyuk Chul Kwon,[†] Tae Gyung Hyung,[†] Kyung Hwa Choi,[†] Sun Wha Oh,[†] Shaorong Yang,[‡] Zhiming Zhao,[‡] and Patrick S. Mariano*[,‡]

Contribution from the Department of Chemistry and the Institute for Functional Materials, Pusan National University, Pusan 609-735, Korea, and Department of Chemistry, University of New Mexico, Albuquerque, New Mexico 87131

Received October 2, 2003; E-mail: mariano@unm.edu

Abstract: The results of studies designed to obtain information about the factors that control the chemical efficiencies/regioselectivities and quantum yields of single electron transfer (SET)-promoted reactions of acceptor−polydonor systems are reported. Photochemical and photophysical investigations were carried out with bis-donor tethered phthalimides and naphthalimides of general structure *N*-phthalimido- and *N*-naphthalimido-CH_2CH_2-D-CH_2CH_2-$NMsCH_2$-E (E = $SiMe_3$ or CO_2NBu_4 and D = NMs, O, S, and NMe). These substrates contain common terminal donor groups ($NMsCH_2SiMe_3$ or $NMsCH_2CO_2NBu_4$) that have known oxidation potentials and cation radical fragmentation rates. Oxidation potentials and fragmentation rates at the other donor site in each of these substrates are varied by incorporating different heteroatoms and/or substituents. Photoproduct distribution, reaction quantum yield, and fluorescence quantum yield measurements were made. The results show that photocyclization reactions of α-trimethylsilylmethansulfonamide (E = $SiMe_3$)- and α-carboxymethansulfonamide (E = CO_2NBu_4)-terminated phthalimides and naphthalimides that contain internal sulfonamide, ether, and thioether donor sites (D = NMs, O, or S) are chemically efficient (80−100%) and that they take place exclusively by a pathway involving sequential photoinduced SET (zwitterionic biradical desilylation or decarboxylation) biradical cyclization. In contrast, photoreactions of α-trimethylsilylmethansulfonamide- and α-carboxymethansulfonamide-terminated phthalimides and naphthalimides that that contain an internal tertiary amine donor site (D = NMe) are chemically inefficient and follow a pathway involving α-deprotonation at the tertiary amine radical cation center in intermediate, iminium radical-containing, zwitterionic biradicals. In addition, the quantum efficiencies for photoreactions of α-trimethylsilylmethansulfonamide- and α-carboxymethansulfonamide-terminated phthalimides are dependent on the nature of the internal donor (eg., $\phi = 0.12$ for D = NMs, E = $SiMe_3$; $\phi = 0.02$ for D = S, E = $SiMe_3$; $\phi = 0.04$ for D = NMe, E = $SiMe_3$). The results of this effort are discussed in terms of how the relative energies of interconverting zwitterionic biradical intermediates and the energy barriers for their α-heterolytic fragmentation reactions influence the chemical yields and quantum efficiencies of SET promoted photocyclization reactions of acceptor−polydonor substrates.

Introduction

A major goal of our past studies in the area of single electron transfer (SET) photochemistry has been the development of novel methods to promote radical and biradical cyclization reactions. These investigations have led to the discovery of several efficient processes, which result in regioselective formation of carbon-centered radicals and biradicals. Examples are found in observations made in our earlier work with allyl- and benzyl-silanes[1−4] which demonstrate that the π-radical cations, generated by SET from these substances to excited-state acceptors, undergo rapid nucleophile-assisted desilylation to produce the corresponding allylic and benzylic radicals or biradicals (Scheme 1). These processes can be incorporated into sequences for the synthesis of structurally complex, natural product targets.[5−7] More recent studies, aimed at developing selective methods for generating carbon-centered radicals based on α-desilylation reactions of nitrogen-centered cation radicals (aminium radicals), uncovered processes which are driven by the formation and reaction of intermediate α-amino and α-amido radicals or biradicals (Scheme 2).[8−11] These transformations take

† Pusan National University.
‡ University of New Mexico.

(1) Ohga, K.; Mariano, P. S. *J. Am. Chem. Soc.* **1982**, *104*, 617.
(2) Ohga, K.; Yoon, U. C.; Mariano, P. S. *J. Og. Chem.* **1984**, *49*, 213.
(3) Borg, R. M.; Heuckeroth, R. O.; Lan, A. J. Y.; Quillen, S. L.; Mariano, P. S. *J. Am. Chem. Soc*. **1987**, *109*, 2728.
(4) Lan, A. J. Y.; Heuckeroth, R. O.; Mariano, P. S. *J. Am. Chem. Soc*. **1987**, *109*, 2738.
(5) Kavash, R. W.; Mariano, P. S. *Tetrahedron Lett*. **1989**, *31*, 4185.
(6) Ho, G. D.; Mariano, P. S. *J. Org. Chem.* **1988**, *53*, 5113.
(7) Ahmed-Schofield, R.; Mariano, P. S. *J. Org. Chem.* **1987**, *52*, 1478.
(8) Hasegawa, E.; Xu, W.; Mariano, P. S.; Yoon, U. C.; Kim, J. U. *J. Am. Chem. Soc.* **1988**, *109*, 8089.
(9) Xu, W.; Zhang, X. M.; Mariano, P. S *J. Am. Chem. Soc.* **1991**, *113*, 8847.
(10) Jeon, Y. T.; Lee, C. P.; Mariano, P. S. *J. Am. Chem. Soc.* **1991**, *113*, 8863.
(11) Yoon, U. C.; Mariano, P. S. *Acc. Chem. Res.* **1992**, *25*, 233.

10.1021/ja0305712 CCC: $27.50

Scheme 1

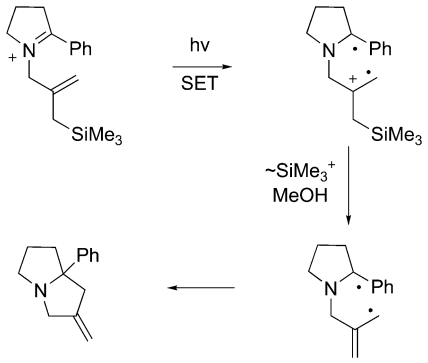

Scheme 2

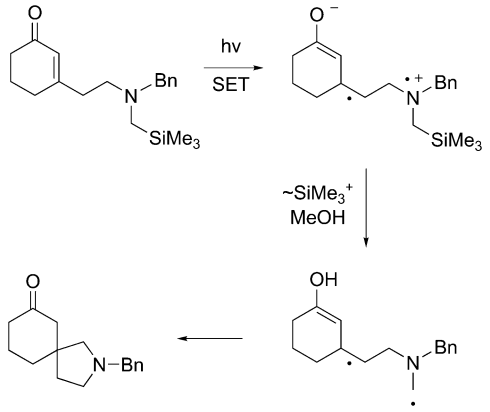

Scheme 3

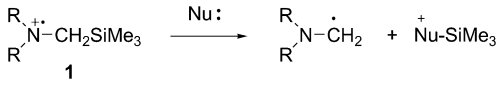

advantage of the high rates of nucleophile assisted desilylation of α-silylaminium radicals **1** for regioselective formation of carbon centered radicals (Scheme 3). Extensive studies have shown that preparative methods based on this chemistry are applicable to the synthesis of a variety of nitrogen-heterocycles.[12,13]

The results of laser flash photolysis studies[14−16] have played a key role in the development of this chemistry by providing important information about the rates of α-silylaminium radical desilylation and how these rates are controlled by silophiles, N-substituents, and media. Perhaps the most significant findings of this effort arose in studies of the dynamics of decay of aminium radicals derived by SET oxidation of α-amino and α-amidosilanes and carboxylates which showed that the rates of bimolecular desilylation and unimolecular decarboxylation of these intermediates far exceed those for a variety of other aminium radical α-fragmentation processes (e.g., deprotonation and retro-aldol cleavage).[16] In addition, the rates of these fast α-fragmentation processes can be further enhanced by placement of electron-withdrawing substituents on nitrogen of the aminium

Scheme 4

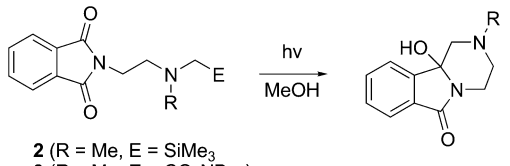

2 (R = Me, E = $SiMe_3$)
3 (R = Me, E = CO_2NBu_4)
4 (R = Ms, E = $SiMe_3$)

radical (eg., as in amide and sulfonamide cation radicals). The high rates of α-decarboxylation of α-aminocarboxylate radical cations and of silophile-assisted α-desilylation of α-silylamide cation radicals are germane to the development of efficient synthetic methods based on SET photochemistry. Examples of this are found in SET-promoted photocyclizations of *N*-aminoethyl-phthalimides **2**−**4** (Scheme 4) where quantum efficiencies are significantly enhanced by changing α-amine substituent E from TMS ($\phi = 0.04$ for **2**)[16] to CO_2NBu_4 ($\phi = 0.32$ for **3**)[16] or the N-substituent from alkyl to methansulfonyl ($\phi = 0.12$ for **4**).[17]

The data accumulated in these investigations also has been used to design efficient SET-induced photomacrocyclization reactions of polyether, polythioether- and polyamide-linked phthalimides (**5**).[18,19] As shown in Scheme 5, irradiation of trimethylsilyl-terminated substrates in these families promotes chemically efficient photocyclization reactions that produce functionalized macrocyclic products. The mechanistic route for these processes involves initial SET from the donor sites in the side chains to the excited phthalimide chromophore, leading to mixtures of intermediate zwitterionic biradicals. In each case, methanol induced desilylation occurs selectively at the terminal cation radical center to produce neutral biradical precursors of the products.

SET-Promoted Photoreactions of Polydonor and Polyacceptor Systems. The structural outcomes and high yields of these photomacrocylization reactions suggest that they will serve as the foundation of practical methods for polyfunctionalized macrocycle synthesis. However, to take full advantage of the preparative potential of this chemistry, an understanding of the factors involved in determining the efficiencies (chemical and quantum yields) and regiochemical selectivities of these reactions must be developed. From a more general perspective, these processes are examples of a broad family of ground- and excited-state redox reactions of polydonor, polyacceptor and linked polydonor−acceptor, or donor−polyacceptor substrates. In systems of these types (exemplified in Scheme 6 by using an intramolecular SET-promoted reaction of an acceptor−bis-donor model) intermolecular or intramolecular SET oxidation or reduction can generate a population of different, perhaps rapidly interconverting, ion radicals, each of which can undergo secondary reactions to generate intermediate radicals or biradicals in pathways leading to product formation. This situation is similar to the coupled electron hopping−chemical reaction

(12) Jung, Y. S.; Swartz, W. H.; Xu, W.; Mariano, P. S.; Green, N. J.; Schultz, A. G. *J. Org. Chem.* **1992**, *57*, 6037.
(13) Khim, S. K.; Mariano, P. S. *Tetrahedron Lett.* **1993**, *35*, 999.
(14) Zhang, X. M.; Yeh, S. R.; Hong, S.; Freccero, M.; Albini, A.; Falvey, D. E.; Mariano, P. S. *J. Am. Chem. Soc.* **1994**, *116*, 4211.
(15) Su Z.; Falvey, D. E.; Yoon, U. C.; Mariano, P. S. *J. Am. Chem. Soc.* **1997**, *119*, 5261.
(16) Su Z.; Falvey, D. E.; Yoon, U. C.; Oh, S. W.; Mariano, P. S. *J. Am. Chem. Soc.* **1997**, *120*, 10676.
(17) Yoon, U. C.; Kim, J. W.; Ryu, J. Y.; Cho, S. J.; Oh, S. W.; Mariano, P. S. *J. Photochem. Photobiol., A* **1997**, *106*, 145.
(18) Yoon, U. C.; Oh, S. W.; Lee, J. H.; Park, J. H.; Kang, K. T.; Mariano, P. S. *J. Org. Chem.* **2001**, *66*, 939.
(19) Yoon, U. C.; Jin, Y. X.; Oh, S. W.; Park, C. H.; Park, J. H.; Campana, C. F.; Cai, X.; Duesler, E. N.; Mariano, P. S. *J. Am. Chem. Soc.* **2003**, *125*, 10664.

Scheme 5

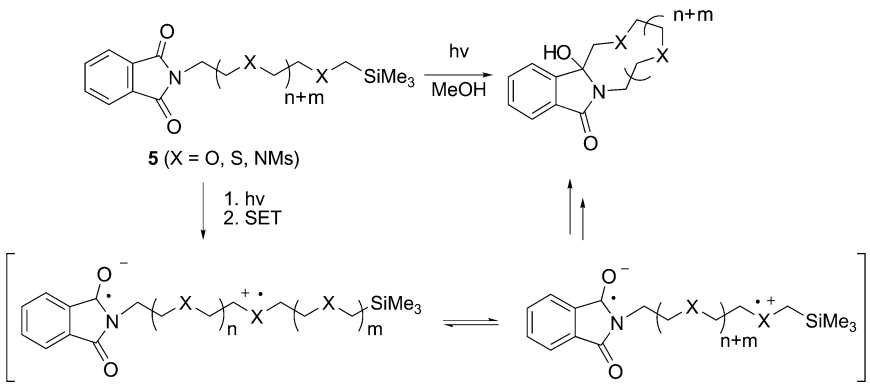

Scheme 6

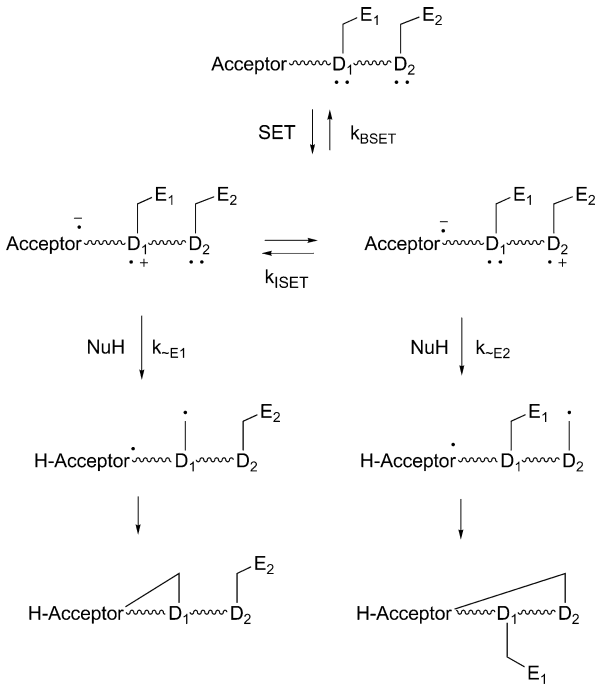

processes that occur in biological macromolecules such as DNA, recently studied by Lewis,[20] Schuster,[21] Giese,[22] and others.

In photoreactions of the acceptor−bis-donor substrate shown in Scheme 6, several factors can contribute in controlling the chemical and quantum yields as well as regiochemical selectivities. First, in cases where intrasite SET (k_{ISET}) is slow compared to the cation radical fragmentation reactions ($k_{\sim E}$), product ratios will be governed by the relative rates of (1) SET from the respective donor sites, and (2) fragmentation versus back SET. In another limiting situation where intrasite SET is faster than reaction at the cation radical centers, an equilibrium mixture of the zwitterionic biradicals will be generated in which the mole fraction of each is governed by the redox potential at each donor site. In this situation, the chemical efficiencies for formation of each of the products will be dependent on the relative rates of the competing fragmentation reactions because the energy barriers for these processes are higher than that for intrasite SET. This is analogous to processes that adhere to the Curtin-Hammett principle,[23] where product ratios arising from rapidly equilibrating reactants are governed by the relatively slower rates of their respective reactions. More complex situations exist in cases when k_{ISET} and $k_{\sim E}$ are in the same range or where intrasite SET is slower than cation radical fragmentations.

The reasoning outlined above leads to the prediction that the efficiencies of redox reactions of polyacceptor and polydonor systems could depend on the number, types, location, and reactivity of ion radical centers formed by either direct or intrasite SET. Clearly, knowledge about how these factors govern product yields, regiochemical selectivities, and quantum efficiencies is crucial to the design of synthetically useful redox reactions of polyfunctionalized substances. As part of a long-range plan designed to obtain information about these issues, we initiated studies with substrates composed of bis-donor side chains linked to light-absorbing phthalimide and naphthalimide acceptors. To determine how zwitterionic biradical energies and α-fragmentation rates govern the chemical yields and quantum efficiencies of photocyclization reactions, a series of phthalimides and 2,3-naphthalimides containing a variety of N-linked donor sites have been prepared and subjected to photochemical study. Common donor groups ($NMsCH_2SiMe_3$ or $NMsCH_2CO_2$-NBu_4) with known oxidation potentials and rates of cation radical fragmentation are incorporated at the terminal position in each of these substrates. Oxidation potentials and fragmentation rates at the other donor sites in these substances are varied by using different heteroatoms and/or substituents.

Results arising from product distribution, reaction quantum yield and fluorescence quantum yield studies with these substrates provide interesting information about how the relative energies of zwitterionic biradicals and the energy barriers for their α-heterolytic fragmentation reactions influence the chemical yields and quantum efficiencies of SET promoted photocyclization reactions of acceptor−polydonor linked systems.

Results

Substrate Synthesis. Two general procedures were used to prepare the TMS-containing polydonor linked phthalimides **14**−**18** (Table 1) and 2,3-naphthalimides **27**−**33** (Table 2), which were employed in the photochemical and photophysical investigations described below. One method involves N-alkylation reactions of the phthalimide or 2,3-naphthalimide anions with the corresponding methanesulfonates or iodides. The other

(20) Lewis, F. D.; Liu, X.; Liu, J.; Miller, S. E.; Hayes, R. T.; Wasielewski, M. R. *Nature* **2000**, *406*, 51.
(21) Sartor, V.; Boone, E.; Schuster, G. B. *J. Phys. Chem. B* **2001**, *105*, 11057.
(22) Giese, B. *Curr. Opin. Chem. Biol.* **2001**, *6*, 612.
(23) Curtin, D. Y. Stereochemical Control of Organic Reactions. *Record Chem. Progr.* (Kresge-Hooker Sci. Lib.) **1954**, *15*, 111.

Table 1. Synthesis of Donor-Tethered Phthalimides

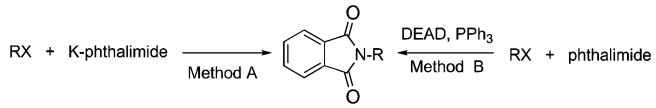

alcohol, mesylate phthalimide, or iodide		R	derivative	method	yield (%)
6	(X = OH)	$CH_2CH_2NMeCH_2CH_2NMsCH_2TMS$	**14**	B	74%
7	(X = OH)	$CH_2CH_2SCH_2CH_2NMsCH_2TMS$	**15**	B	90%
8	(X = OMs)	$CH_2CH_2OCH_2CH_2NMsCH_2TMS$	**16**	A	47%
9	(X = OMs)	$CH_2CH_2OCH_2CH_2NAcCH_2TMS$	**17**	A	63%
10	(X = OMs)	$CH_2CH_2OCH_2CH_2OCH_2CH_2NMsCH_2TMS$	**18**	A	21%
11	(X = I, Z = Et)	$CH_2CH_2NMsCH_2CO_2Z$	**19** (Z = H)	A	81%
12	(X = I, Z = Et)	$CH_2CH_2OCH_2CH_2NMsCH_2CO_2Z$	**20** (Z = H)	A	19%
13	(X = OH, Z = Et)	$CH_2CH_2NMeCH_2CH_2NMsCH_2CO_2Z$	**21** (Z = H)	B	25%

Table 2. Synthesis of Donor-Tethered 2,3-Naphthalimides

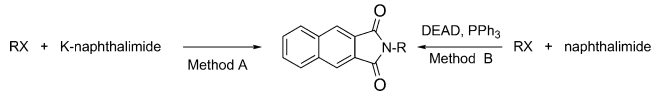

alcohol, mesylate, or iodide		R	naphthalimide derivative	method	yield (%)
22	(X = OMs)	$CH_2CH_2NMsCH_2TMS$	**27**	A	83
23	(X = OMs)	$CH_2CH_2NMsCH_2CH_2NMsCH_2TMS$	**28**	A	74
8	(X = OMs)	$CH_2CH_2OCH_2CH_2NMsCH_2TMS$	**29**	A	80
24	(X = OH)	$CH_2CH_2NMeCH_2TMS$	**30**	B	90
6	(X = OH)	$CH_2CH_2NMeCH_2CH_2NMsCH_2TMS$	**31**	B	67
10	(X = OMs)	$CH_2CH_2OCH_2CH_2OCH_2CH_2NMsCH_2TMS$	**32**	A	34
9	(X = OMs)	$CH_2CH_2OCH_2CH_2NAcCH_2TMS$	**33**	A	60
11	(X = I, Z = Et)	$CH_2CH_2NMsCH_2CO_2Z$	**34** (Z = H)	A	34
26	(X = OH, Z = Et)	$CH_2CH_2NMeCH_2CO_2Z$	**35** (Z = H)	B	34
13	(X = OH, Z = Et)	$CH_2CH_2NMeCH_2CH_2NMsCH_2CO_2Z$	**36** (Z = H)	B	33

procedure takes advantage of Mitsunobo coupling[24] of phthalimide or 2,3-naphthalimide with the appropriate alcohols. Similar routes were used to prepare the carboxylic acid-terminated phthalimides **19**−**21** and naphthalimides **34**−**36** (Tables 1 and 2). In these cases, N-alkylation or Mitsunobo coupling reactions of ethyl ester derivatives of the corresponding methanesulfonates, iodides, and alcohols were followed by ester hydrolysis to produce the target carboxylic acids.

Preparative Photochemistry of Polydonor-Linked Phthalimides. Preparative photochemical reactions of the phthalimide and 2,3-naphthalimide derivatives were investigated to determine how (1) the number, nature, and position of the donor sites and (2) the type of cation radical α-heterolytic fragmentation process controls the yields and regioselectivities of the SET-promoted photocyclization processes. In earlier studies,[18] we had shown that the TMS-terminated phthalimido bis-sulfonamide **37** undergoes highly efficient cyclization to produce the corresponding cyclic amidol **38** (Scheme 7) when irradiated in MeOH by using Pyrex glass filtered light (λ > 290 nm). In the current effort, we observed that the ether- and thioether-bridged α-silylsulfonamides **15**, **16**, and **18** and bridged α-silylacetamide **17** react efficiently to generate the respective amidols **39**−**42** under these photochemical conditions. In contrast, irradiation of a MeOH solution of the amine-sulfonamide **14** leads to formation of a complex mixture of substances consisting of noncyclized products **43**−**44** and cyclic amidol **45** (Scheme 8). To demonstrate that the tertiary amine group in **14** is responsible for its unselective photochemical behavior, a MeOH solution of this phthalimide containing 0.02 M $HClO_4$ was irradiated. Under these conditions, where the tertiary amine group is protonated, the amidol **46** and amido ether **47** (from **46** by acid-catalyzed MeOH exchange) are cleanly generated (Scheme 9).

Scheme 7

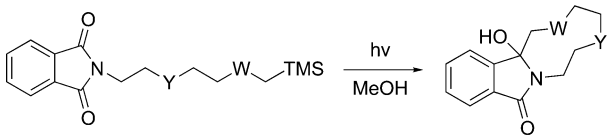

37 (Y = W = NMs)
15 (Y = S, W = NMs)
16 (Y = O, W = NMs)
17 (Y = O, W = NAc)
18 (Y = OCH_2CH_2O, W = NMs)

38 (91%)
39 (97%)
40 (91%)
41 (93%)
42 (89%)

In our earlier LFP studies,[14−16] we demonstrated that decarboxylation of aminum radicals takes place more rapidly than MeOH-promoted desilylation. To determine if this rate difference influences the efficiencies and regioselectivities of photocyclization reactions of polydonor phthalimides, the photochemistry of tetrabutylammonium carboxylate derivatives of acids **19**, **20**, and **21** was explored. Irradiation of the in situ generated tetrabutylammonium carboxylates of **19** and **20** in MeOH leads to efficient formation of the corresponding cyclic amidols **48** and **40** (Scheme 10). In contrast, irradiation of the tetrabutylammonium salt of *N*-methyl-*N*-silylmethylmethansulfonamide **21** results in production of a mixture of carboxylate-containing products along with the cyclic amidol **46**, the product formed by operation of a sequential SET-decarboxylation pathway.

Preparative Photochemistry of Polydonor-Linked 2,3-Naphthalimides. The photochemical properties of polydonor-

(24) Mitsunobo, O. *Synthesis* **1981**, 1.

Scheme 8

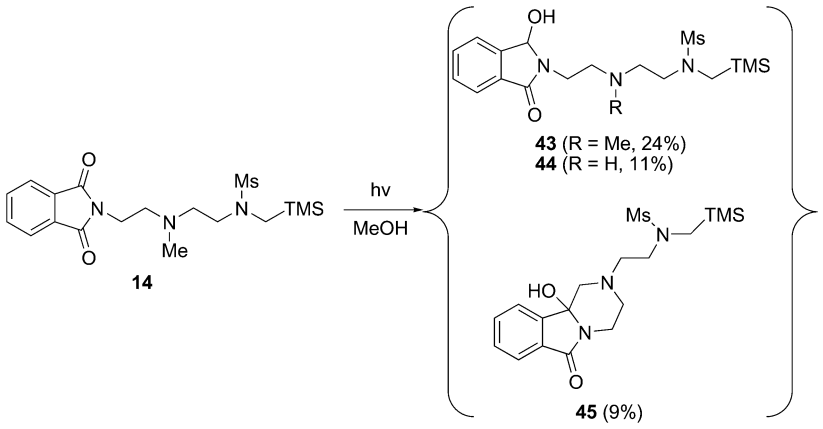

Scheme 9

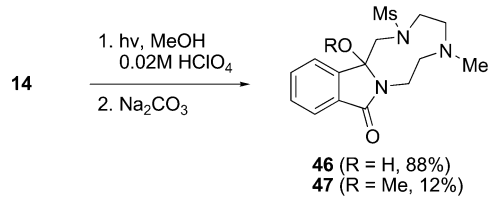

Scheme 10

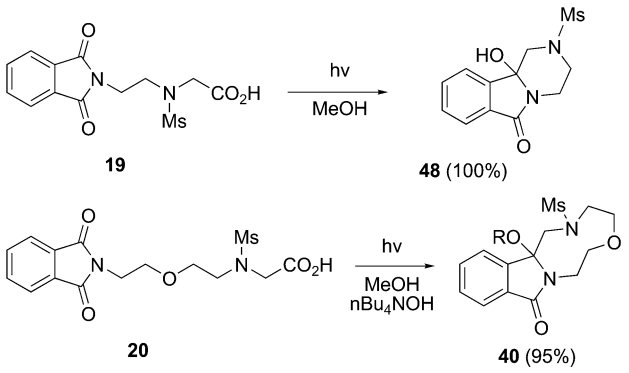

Scheme 11

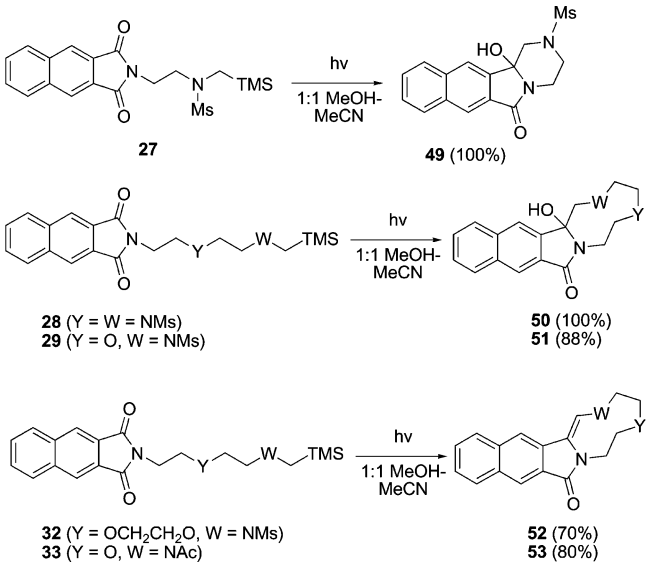

Scheme 12

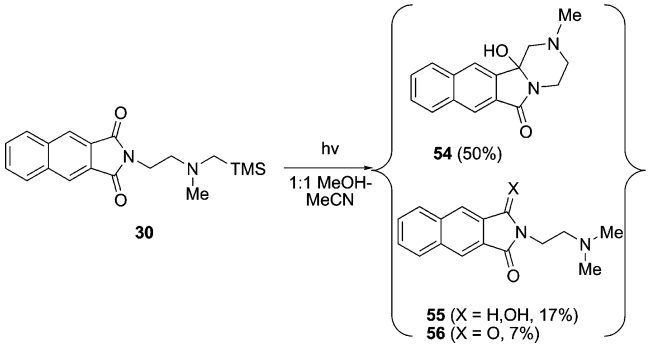

linked 2,3-naphthalimide derivatives closely parallel those of the phthalimide analogues. For example, the TMS-terminated naphthalimido-sulfonamides and acetamides **27**−**29** and **32**−**33** are converted to the respective cyclic amidols (**49** and **50**−**51**) and enamides (**52** and **53**) in high yields when irradiated in 1:1 MeOH−MeCN (Scheme 11). In contrast the related amine derivative **30** reacts to produce a mixture of amidols **54** and **55**, and phthalimide **56** under these photochemical conditions (Scheme 12). Also, irradiation of a 1:1 MeOH−MeCN solution of the amine sulfonamide **31** leads to formation of the TMS-containing product **57** and cyclic amidol **58** (Scheme 13). Here again, blocking the donor ability of the amine function by protonation alters the photochemical process. Accordingly, irradiation of **31** in 1:1 MeOH−MeCN containing 0.02 M $HClO_4$ promotes efficient formation of either the enamide **59** or a mixture of cyclic amidol **60** and methyl ether **61**, depending upon whether neutralization is performed before or after concentration of the photolysate (Scheme 14).

Again paralleling the behavior of the phthalimide analogues, irradiation of the naphthalimido-carboxylate derivative of sulfonamide **34** leads to clean generation the cyclic amidol **49** (Scheme 15). In contrast, photoreaction of the in situ generated carboxylate derivative of amine **35** produces a mixture of the amidol **54** and *N*,*N*-dimethylnaphthalimide **56** (Scheme 16). Finally, irradiation of the in situ formed amine-sulfonamidocarboxylate **36** leads to formation of a complex mixture of products, in which the cyclic amidol **60** is only a minor component (Scheme 16).

Photoreaction Quantum Efficiencies. To gain preliminary information about the factors that contribute in determining the quantum efficiencies of these processes, the quantum yields for disappearance of the donor-linked phthalimides **14**−**21** and **37** were measured (Table 3). The actinometers used for this purpose are the TMS- and carboxylate-terminated phthalimido-amines and -sulfonamide **2**−**4**.[16,17] The results of these measurements

Scheme 13

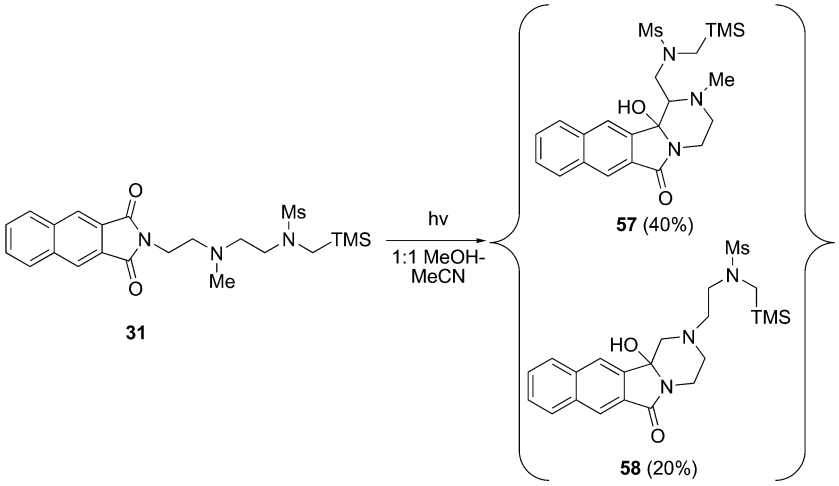

Scheme 14

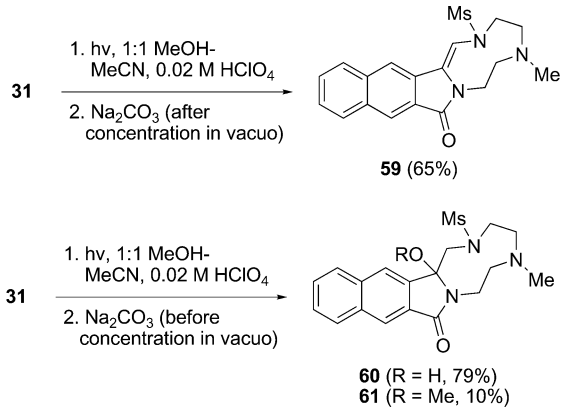

Scheme 15

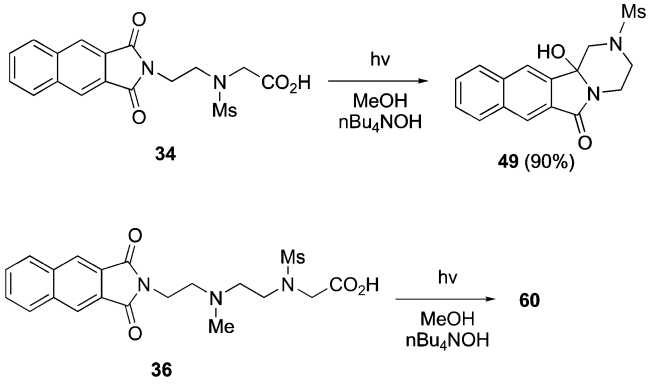

are summarized in Table 3. In addition, the relative quantum yields for irradiation induced disappearance of selected naphthalimide derivatives **27**−**31** were determined to evaluate substrates, for which fluorescence emission efficiency data can be obtained (Table 4). Here, the relative quantum yields are given relative to that for the silylsulfonamido-naphthalimide **27**.

Fluorescence Quantum Yields. The initial rates of SET from donor sites in the side chains to the excited states of the phthalimide and naphthalimide chromophores should play a role in governing the population of initially formed zwitterionic biradical intermediates. Consequently, we have used fluorescence spectroscopy to gain information about how the intramolecular SET rates vary with the number, nature, and location of donor sites. Because 2,3-naphthalimide chromophore is strongly

Scheme 16

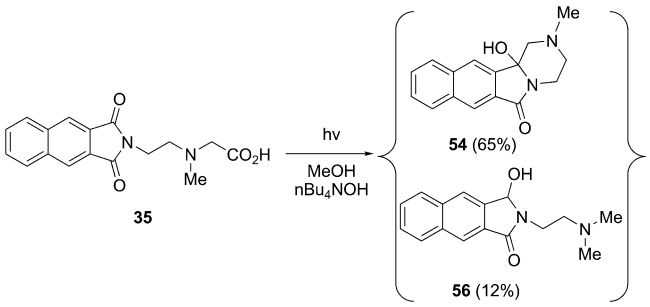

fluorescent,[25−27] the emission quantum yields of donor-linked naphthalimides provide a direct method to measure the rates of intramolecular SET. Thus, by using the fluorescence quantum yield data and the known intrinsic singlet lifetime of *N*-methyl-2,3-naphthalimide (6.6 ns),[26] the rate constants for SET from side-chain donors to the naphthalimide singlet excited states can be calculated. The fluorescence quantum yield and intramolecular SET rate data gained from studies with selected donor-linked naphthalimdes are given in Table 5. The data show that rate constants for SET from the tertiary amine donor sites in **30**, **31**, and **36** to the singlet excited naphthalimide chromophore fall in the range of $(2-4) \times 10^9$ s^{-1}. The 1 order of magnitude larger rate constant for intramolecular SET in the tertiary aminocarboxylate-containing naphthalimide **35** is likely due to the aminium radical-stabilizing effect of the α-carboxylate group which results in lowering the oxidation potential of the amine donor.[27]

Discussion

Mechanistic Analysis. The results of the investigations described above provide a foundation for understanding some of the factors that govern the chemical yields and quantum efficiencies of SET-promoted photoreactions of acceptor−polydonor systems. Photochemical reactions of substrates probed in this effort are initiated by SET from side-chain donor sites to excited states of the phthalimide and 2,3-naphthhalimide

(25) Valat, P.; Wintgens, V.; Kossanyi, J.; Biczok, L.; Demeter, A.; Berces, T. *J. Am. Chem. Soc.* **1992**, *114*, 946.
(26) Wintgens, V.; Valat, P.; Kossanyi, J.; Biczok, L.; Demeter, A.; Berces, T. *J. Chem. Soc., Faraday Trans.* **1994**, *90*, 411.
(27) Demeter, A.; Berces; Biczok, L.; Wintgens, V.; Valat, P.; Kossanyi, J. *J. Chem. Soc., Faraday Trans.* **1994**, *90*, 2635.

Table 3. Quantum Yields for Photoreactions of the Donor Linked[a]

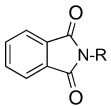

phthalimide derivative	R	disappearance quantum yields[a]
2	$CH_2CH_2NMeCH_2TMS$	0.04 (ref 16)
3	$CH_2CH_2NMeCH_2CO_2NBu_4$	0.32 (ref 16)
4	$CH_2CH_2NMsCH_2TMS$	0.12 (ref 17)
14	$CH_2CH_2NMeCH_2CH_2NMsCH_2TMS$	0.04 ± 0.03
14-H	$[CH_2CH_2NHMeCH_2CH_2NMsCH_2TMS]^+$	0.34 ± 0.12
15	$CH_2CH_2SCH_2CH_2NMsCH_2TMS$	0.02
16	$CH_2CH_2OCH_2CH_2NMsCH_2TMS$	0.14 ± 0.01
17	$CH_2CH_2OCH_2CH_2CH_2CH_2NAcCH_2TMS$	0.10
18	$CH_2CH_2CH_2CH_2OCH_2CH_2CH_2CH_2OCH_2CH_2CH_2NMsCH_2TMS$	0.13 ± 0.01
19	$CH_2CH_2CH_2NMsCH_2CO_2NBu_4$	0.21 ± 0.01
20	$CH_2CH_2CH_2CH_2CH_2OCH_2CH_2NMsCH_2CO_2NBu_4$	0.39 ± 0.07
21	$CH_2CH_2NMeCH_2CH_2CH_2CH_2NMsCH_2CO_2NBu_4$	0.02
37	$CH_2CH_2CH_2CH_2NMsCH_2CH_2NMsCH_2CH_2TMS$	0.12 ± 0.01

[a] See Experimental Section for a description of the procedure used to determine the quantum yields for substrate disappearance.

Table 4. Relative Quantum Yields for Photoreaction of the Donor-Linked 2,3-Naphthalimide

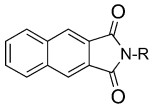

naphthalimide derivative	R	relative disappearance quantum yields[a]
27	$CH_2CH_2NMsCH_2TMS$	1
28	$CH_2CH_2NMsCH_2CH_2^{NMs}CH_2TMS$	0.58
29	$CH_2CH_2OCH_2CH_2CH_2CH_2CH_2NMsCH_2TMS$	0.44
30	$CH_2CH_2CH_2CH_2NMeCH_2CH_2CH_2TMS$	0.02
31	$CH_2CH_2CH_2CH_2NMeCH_2CH_2NMsCH_2CH_2CH_2TMS$	0.07

[a] See Experimental Section for a description of the procedure used to determine the quantum yields for substrate disappearance.

Table 5. Quantum Yields for Fluorescence and Calculated Intramolecular-SET Rate Constants (*k* SET) for the Donor Linked 2,3-Naphthalimides

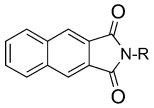

naphthalimide derivative	R	fluorescence quantum yields	*k* (SET)[a] 1×10^{-9} s^{-1}
–	Me	0.30 (ref 23)	–
28	$CH_2CH_2CH_2CH_2NMsCH_2CH_2NMsCH_2CH_2TMS$	0.22	0.06
30	$CH_2CH_2CH_2CH_2NMeCH_2TMS$	0.01	4
31	$CH_2CH_2CH_2CH_2NMeCH_2CH_2NMsCH_2TMS$	0.02	2
31-H	$[CH_2CH_2NHMeCH_2CH_2NMsCH_2TMS]$	0.28	0.01
32	$CH_2CH_2OCH_2CH_2OCH_2CH_2NMsCH_2TMS$	0.28	0.01
35	$CH_2CH_2NMeCH_2CO_2NBu_4$	0.002	23
35-H	$CH_2CH_2NHMeCH_2CH_2CH_2CO_2$	0.15	0.2
36	$CH_2CH_2NMeCH_2CH_2CH_2CH_2CH_2NMsCH_2CO_2NBu_4$	0.01	4
36-H	$CH_2CH_2CH_2CH_2CH_2NHMeCH_2CH_2CH_2NMsCH_2CO_2$	0.23	0.05

[a] Calculated by using the assumption that the intrinsic singlet lifetimes of the 2,3-naphthalimide chromophoresin the donor-linked substrates are the same as that of for *N*-methyl-2,3-naphthalimide (6.6 ns, ref 23).

chromophores. This process (Scheme 17) gives rise to a mixture of zwitterionic biradicals, **62** and **63**. The relative populations of the zwitterionic biradicals (**62** vs **63**), produced from the bis-donor substituted phthalimides and naphthalimides, can be governed by either the relative rates of their formation by intramolecular SET or their relative energies if intrasite SET is faster than the ensuing heterolytic fragmentation reactions. Specifically, in the cases where intrasite SET takes place more rapidly than other decay pathways, the relative energies of the zwitterionic biradicals, which are related to the oxidation potentials at each donor site, will control their populations. Zwitterionic biradicals **62**−**63** can participate in one or more competitive processes involving (1) back-SET to generate ground-state substrates, (2) proton transfer from internal cation radical sites to the carbonyl oxygen of phthalimide anion radicals, and (3) MeOH-promoted desilylation or unimolecular decarboxylation at the terminal sulfonamide cation radical center. The heterolytic fragmentation reactions ($\sim H^+$, $\sim SiMe_3^+$, and $-CO_2$) produce biradicals, **64** and **65**, which either react to form cyclic amidols or other typical products of disproportionation.

Trends Observed. Although we expect that intrasite SET will be fast,[29] no data is currently available about this issue. In contrast, the relative rates of intramolecular SET from the donor

Scheme 17

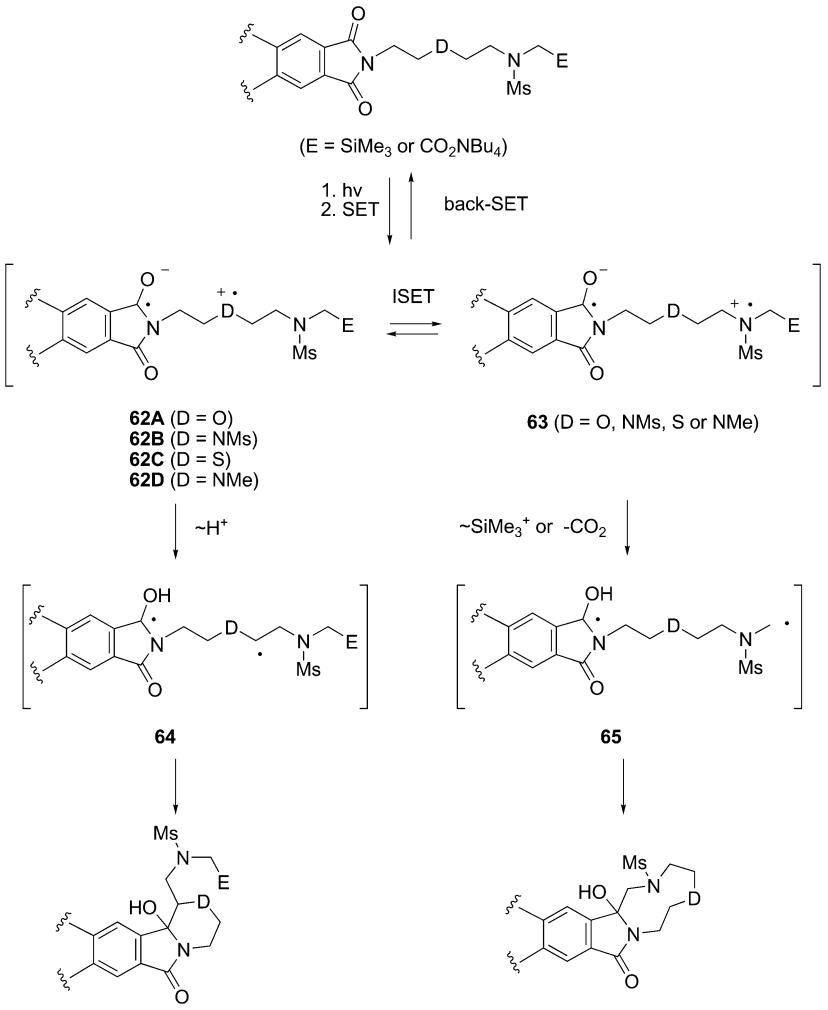

sites in the bis-donor-substituted naphthalimides can be estimated by using emission spectroscopic methods. Accordingly, a comparison of the fluorescence quantum yields for mono- and bis-donor-substituted 2,3-naphthalimides to that of a nondonor-containing model compound gives a direct measurement of the intramolecular SET rate constants. The model used for this purpose is *N*-methyl-2,3-naphthalimide, whose fluorescence quantum yield (0.30) and singlet lifetime (6.6 ns) have been determined previously.[26] The two reasonable assumptions made in deriving k_{SET} data by using this procedure is that (1) singlet quenching follows an SET pathway, and (2) the intrinsic singlet lifetimes of the 2,3-naphthalimide chromophore are identical in the *N*-methyl and the donor-linked substrates. As can be seen by viewing the kinetic data given in Table 5, the intramolecular-SET rate constants (k_{SET}) vary over a range of 3 orders of magnitude and are directly dependent on the electron-donating ability (inversely related to oxidation potentials) of the donor sites in the naphthalimide side chains. For example, k_{SET} values from tertiary amine centers in naphthalimides **30**, **31**, and **36** range from 2 to 4 $\times$ 10^9 s^{-1}. As expected, protonation blocks intramolecular SET in the singlet excited states of these substrates. In contrast, SET from α-silyl- or α-carboxy-sulfonamide donor sites occurs more slowly with k_{SET} values ranging from 1 $\times$ 10^8 s^{-1} (for **28** and protonated **36**) to 1 $\times$ 10^7 s^{-1} (for bis-ether **32** and protonated **31**).

The results show that the rates of intramolecular SET from the donor sites in the linked naphthalimides parallel those predicted by using simple free energy calculations. Accordingly, SET from the tertiary amine centers ($E_{1/2}(+)$ = ca. 0.6 V) to the singlet excited 2,3-naphthalimide chromophore ($E_{1/2}{}^{S}1(-)$ = ca. 1.8 V)[30] is highly exothermic in contrast to SET from more weakly donating sulfonamide ($E_{1/2}(+)$ = ca. 2 V)[17,31] and ether ($E_{1/2}(+)$ = ca. 2 V)[32] donors. As a consequence, the relative populations of zwitterionic biradicals, formed by intramolecular excited-state electron transfer, should be biased in favor of those that contain lower-energy cation radical sites. It is important to note that intramolecular SET rates could also display a distance dependence. This factor has not been probed in the current investigation.

(28) Oxidation potentials of tertiary amines are significantly lower than that of carboxylates. Thus, SET from the carboxylate to the excited naphthalimide chromophore is not likely. Confirmation of this proposal is found in LFP studies (ref 16) of α-aminocarboxylate-derived cation radicals.

(29) See: Oevering, H.; Paddon-Row, M. N.; Heppener, M.; Oliver, A. M.; Cotsaris, E.; Verhoeven, J. W.; Hush, N. S. *J. Am. Chem. Soc.* **1987**, *109*, 3258, Yonemoto, E. H.; Saupe, G. B.; Schnehl, R. H.; Hubig, S. M.; Riley, R. L.; Iverson, B. L.; Mallouk, T. E. *J. Am. Chem. Soc.* **1994**, *116*, 4786 and references therein.

(30) Somich, C.; Mazzocchi, P. H.; Edwards, M.; Morgan, T.; Ammon, H. L. *J. Org. Chem.* **1990**, *55*, 2624.

(31) Shono, T.; Matsumura, Y.; Tsubata, K.; Uchida, K.; Kanazawa, T.; Tsuda, K. *J. Org. Chem.* **1984**, *49*, 3711.

(32) Estimated on the basis of oxidation potentials of alcohols given in Lund, H. *Acta Chem. Scand.* **1957**, *11*, 491.

Observation made in studies of preparative photochemical reactions of the α-silyl- and α-carboxy-sulfonamide-terminated substrates suggest the existence of several interesting trends. First, members of the sulfonamido-phthalimide and -naphthalimide families, which contain other heteroatom donor sites (e.g., O, NMs) that have higher or nearly equal oxidation potentials than the terminal sulfonamide, undergo chemically efficient/highly regioselective photocyclization reactions via sequential SET-desilylation or SET-decarboxylation pathways. Examples of this pattern are found in photocyclization reactions of phthalimides **16**−**18**, **20**, and **37**, and naphthalimides **28**−**33**. Second, α-silyl- and α-carboxy-sulfonamide substrates **14**, **21**, **31**, and **36**, which possess an internal, strongly electron-donating tertiary amine site, undergo low yielding unselective photoreactions. In these cases, exemplified by the amino-sulfonamides **14** and **31**, the major pathway followed involves α-proton transfer from the internal tertiary aminium radical centers followed biradical cyclization or disproportionation. Finally, the thioether containing phthalimido-sulfonamide **15** represents an intermediary case where highly efficient photocyclization takes place via a sequential SET-desilylation route despite the presence of a sulfur donor site that has a significantly lower oxidation potential than the terminal α-silylsulfonamide.

Factors Governing Photocyclization Reaction Efficiencies. These observations suggest that at least two factors participate in governing the chemical efficiencies/regioselectivities of photocyclization reactions of the bis-donor linked, α-silylsulfonamide-terminated phthalimides and naphthalimides. The first contribution comes from the relative intrinsic rates of the competitive α-heterolytic fragmentation processes ($\sim H^+$, $\sim SiMe_3^+$, $-CO_2$) which can occur at each cation radical site in the mixture of zwitterionic biradicals. A second input comes from the relative energies of the zwitterionic biradicals, which control both their initial and final populations and which can influence the actual energy barriers for the competing α-heterolytic fragmentation processes. In accord with this line of reasoning, fast α-desilylation and α-decarboxylation at the sulfonamide sites of terminal zwitterionic biradicals **63** (Scheme 17) are the dominant reaction pathways followed when the nonterminal zwitterionic biradical counterparts **62**, which can only undergo slow α-deprotonation, are of near equal or higher energy than **63**. An important conclusion drawn from this analysis is that the rates of intrasite SET in the zwitterionic biradicals with NMs, O, and S donor sites must be faster than desilylation or decarboxylation at the terminal sulfonamide cation radical centers. However, when the energies of the internal zwitterionic biradicals **62** are significantly lower than those of their terminal α-silylsulfonamide counterparts **63**, pathways involving α-deprotonation at the internal cation radical site can predominate. In these cases, intrasite SET must take place more slowly than cation radical deprotonation, desilylation, or decarboxylation.

Additional information, leading to a proposed framework for understanding how zwitterionic biradical energies and fragmentation rates govern the nature of efficiencies of SET-promoted photoreactions of acceptor−polydonor substrates, comes from the results of reaction quantum yield studies. An analysis of the mechanistic sequence presented in Scheme 17 shows that the quantum efficiencies for reactions of the bis-donor substrates should depend on the relative rates of reaction pathways which compete with back-SET for deactivation of the zwitterionic biradical intermediates. Importantly, the fraction of the biradical intermediates, which proceed to form products, is dependent on the combined rates of α-deprotonation, α-desilylation, and α-decarboxylation as compared to that for back-SET. Also, depending on whether intrasite SET is faster or slower than other zwitterionic biradical decay pathways, the equilibrium constants for interconversion of these intermediates will also be a factor in governing reaction quantum yields.

Scheme 18

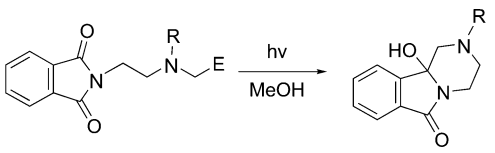

Phthalimide	R	E	ϕ
66	Me	H	0.003[a]
67	Ac	H	0.025[a]
2	Me	$SiMe_3$	0.038a
68	Ac	$SiMe_3$	0.12 a
4	Ms	$SiMe_3$	0.12 b
3	Me	CO_2NBu_4	0.32 a
69	Ac	CO_2NBu_4	0.40 a
19	Ms	CO_2NBu_4	0.21 c

(a) ref. 16; (b) ref. 17; (c) this work

When viewed in this manner, the quantum yield data from studies of the α-carboxy- and α-silyl-sulfonamide-terminated phthalimides, provide information about how the energies and fragmentation rates of zwitterionic biradicals influence the photochemical behavior of acceptor−polydonor substrates. In this and previous studies,[16,17] we have shown that the quantum yields for photocyclization reactions of aminoethyl-phthalimide derivatives vary in a regular manner with the nature of the α-electrofugal group (E = H, TMS, or CO_2NBu_4) and nitrogen substituent (R = Me, Ac, or Ms). These data (Scheme 18) provide a framework for interpreting the quantum efficiencies of photoreactions of the bis-donor substituted phthalimides (Table 3). Simply stated, the quantum yields for photocyclization reactions of the bis-donor-containing α-silyl- and α-carboxy-phthalimides should be in the range of those for the monosilylsulfonamido- and monocarboxysulfonamido-phthalimides (Scheme 18, **4**, $\phi = 0.12$, and **19**, $\phi = 0.21$, respectively) if the radical cation sites in zwitterionic biradicals, derived from these substances, reside predominantly at the terminal sulfonamide moieties.

Interestingly, this appears to be the case for photoreactions of the silicon-substituted bis-sulfonamide **37** ($\phi = 0.12$), ether-sulfonamide **16** ($\phi = 0.14$), and bis-ether-sulfonamide **18** ($\phi = 0.13$) as well as the carboxylate-terminated either-sulfonamide **20** ($\phi = 0.39$). In dramatic contrast, photoreactions of the α-silyl- and α-carboxy-sulfonamides **14** ($\phi = 0.04$) and **21** ($\phi = 0.02$), both of which contain an internal tertiary amine donor site, proceed with quantum efficiencies that match those of model processes that follow sequential SET−proton-transfer pathways (eg., Scheme 18, **66**, $\phi = 0.003$). This same trend is observed for the relative quantum yields for photocyclization

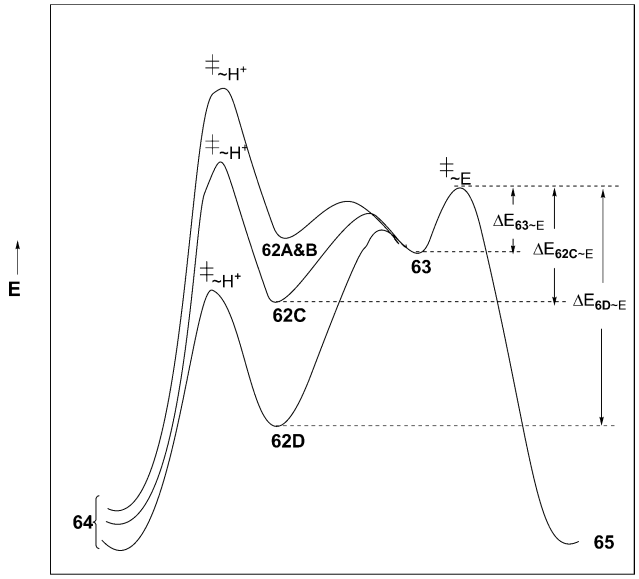

Figure 1. Energy profiles for competing α-deprotonation, α-desilylation, and α-decarboxylation reactions of zwitterionic biradicals **62A**−**D** and **63** serving as intermediates in SET-promoted photochemical reactions of bis-donor-substituted phthalimides. See Scheme 17 for the structures of the zwitterionic biradicals **62A**−**D** and **63** and biradicals **64**−**65**.

reactions of the 2,3-naphthalimides **27**−**30** (Table 4). Moreover, although proceeding with a high chemical yield, photoreaction of the thioether-silylsulfonamide **15** has a much lower quantum efficiency ($\phi = 0.02$) than those of the model monosilyl-sulfonamide (Scheme 18, **4**, $\phi = 0.12$). The results presented above are best accommodated by the energy scheme shown in Figure 1. Assignments of the relative energies of the zwitterionic biradicals, **62A**−**62D** and **63**, which serve as intermediates in photoreactions of the bis-donor-linked phthalimides, are made on the basis of the known oxidation potentials of model ethers (ca. + 2.5 V),[32] methanesulfonamides (ca. + 2.5 V),[31] α-silyl-methanesulfonamides (ca. + 2.0 V),[17] thioethers (ca. + 1.4 V),[33] and tertiary amines (ca. + 0.6 V).[34] In addition, the relative heights of the intrinsic energy barriers for competing α-heterolytic fragmentation reactions ($\sim H^+$, $\sim SiMe_3^+$, $-CO_2$) of the zwitterionic biradicals are estimated by using kinetic data obtained from studies of α-deprotonation, α-desilylation, and α-decarboxylation reactions of tertiary amine- and amide-derived cation radicals.[14−16] Accordingly, activation energies for decarboxylation- and MeOH-induced desilylation are lower than those for deprotonation of amine, thioether, ether, and sulfonamide cation radicals. The kinetic and thermodynamic data lead to the experimentally verified conclusion that reactions of the interconverting mixture of zwitterionic biradicals, **62A**−**63** and **62B**−**63**, formed from the ether-sulfonamides, **16** and **20**, and bis-sulfonamide **37**, will be dominated by α-desilylation or α-decarboxylation leading to **65**. Moreover, in cases where the lowest-energy zwitterionic biradicals **63** which have α-silyl and α-carboxy substituents are also the most reactive, the energy barriers (thus rates) for desilylation or decarboxylation ($\Delta E_{\mathbf{63}\sim E}$) will be nearly the same as those for desilylation and decarboxylation of the zwitterionic biradicals derived from the monosilysulfonamide **4** and monocarboxysulfonamide **19**. Thus, the quantum yields for photocyclization reactions of silylsulfonamide **16** ($\phi = 0.14$) and **37** ($\phi = 0.12$) and carboxysulfonamide **20** ($\phi = 0.39$) should be in the same range as that for the corresponding mono-donor models (Scheme 18, **4**, $\phi = 0.13$ and **19**, $\phi = 0.21$). Importantly, this prediction matches the experimental findings quite well.

The situation is a bit different in the case of the zwitterionic biradicals **62C**−**63** arising from the phthalimido-thioether-sulfonamide **15**. The observation that this substrate undergoes chemically efficient photocyclization by a sequential SET-desilylation pathway suggests that the transition state for desilylation ($\neq_{\sim E}$) of **63** (D = S) is of lower energy than that for α-deprotonation ($\neq_{\sim H}$) at the internal thioether cation radical center in **62C**. The unique and distinguishing feature of the photoreaction of thioether-sulfonamide **15** is that the (apparently) reactive zwitterionic biradical **63** (D = S) is of significantly higher energy (ca. 14 kcal/mol) than the (apparently) unreactive partner **62C**. Although this difference does not influence the chemical yield/regioselectivity of the process, it has a profound effect on the quantum efficiency ($\phi = 0.02$). Specifically, the energy barrier for desilylation of the zwitterionic biradicals **62C**−**63** ($\Delta E_{\mathbf{62C}\sim E}$) is now much greater than that for desilylation of either **62A**−**63** or **62B**−**63** ($\Delta E_{\mathbf{63}\sim E}$). As a result, desilylation is less competitive with back-SET than it is in the cases of zwitterionic biradicals derived from the ether-sulfonamide **16** and bis-sulfonamide **37**.

Photoreactions of the tertiary amine containing α-silyl- and α-carboxy-sulfonamides **14** and **21** represent the third scenario for processes, which proceed via the intermediacy of two or more potentially interconverting zwitterionic biradicals. In these cases, the tertiary aminium radical-containing zwitterionic biradicals **62D** are much lower in energy (ca. 44 kcal/mol) than their sulfonamide cation radical partners **63** (D = NMe). This means that the energy barriers for desilylation and decarboxylation of **62D**−**63** ($\Delta E_{\mathbf{62D}\sim E}$) are insurmountably high. Consequently, photoreactions of these substrates take place by pathways involving slow deprotonation of **62D**. Also, they have the same low quantum efficiencies (**14**, $\phi = 0.04$; **21**, $\phi = 0.02$) as do photoreactions of aminoethyl-phthalimides which take place by sequential SET-deprotonation routes.

Conclusions

It is clear that additional information is needed to solidify and generalize the conclusions presented above. For example, one important conclusion made in the analysis is that intrasite SET in zwitterionic biradicals derived from polydonor-substituted phthalimides can have intrinsically low energy barriers, and as a result, they have rates that are controlled mainly by the energy differences between these potentially equilibrating intermediates. However, to our knowledge, measurements of intrasite SET have not been reported for simple polydonor-derived cation radicals. In addition, an assumption has been made that α-deprotonation reactions of ether- and thioether-derived cation radicals have intrinsic rates/energy barriers that are in the range of those for tertiary aminium radicals. Here again, we know of no studies in which the rates of ether and thioether cation radical deprotonation reactions have been measured.

Despite these limitations, the conclusions drawn from the current studies can serve as a general guide in predicting the chemical yields/regioselectivities and quantum efficiencies of

(33) Cottrell, P. T.; Mann, C. K. *J. Electrochem. Soc.* **1969**, *116*, 1499.
(34) Mann, C. K. *Anal. Chem.* **1964**, *36*, 2424.

SET-promoted photochemical reactions of acceptor−polydonor systems. For example, when the lowest-energy zwitterionic biradical, derived by intramolecular and/or intrasite SET in a substrate of this type, contains the most reactive cation radical site, a highly efficient/regioselective photoreaction will ensue. Also, the quantum efficiency of this process will be in the range of that for a simple acceptor−monodonor model. On the other hand, when the lowest-energy zwitterionic biradical is the least reactive, the photochemical reaction will have a low quantum efficiency and either a high or low chemical yield/regioselectivity, depending on whether the relative energies of the transition states for the competing cation radical fragmentation processes are large or small.

On the basis of these conclusions, it appears that reactions of potentially equilibrating mixtures of zwitterionic biradicals can be understood in terms of the classical Curtin-Hammett principle.[23] In this context, when the rates of zwitterionic biradical interconversion are larger than those for their reactions, the relative energies of the transition states for ensuing reactions of these charged biradicals will govern product distributions (regioselectivities). Also, the overall rates of reaction of the equilibrating mixtures, which influence the quantum yields, will be governed by the energy differences between the lowest-energy zwitterionic biradicals and the lowest energy of transition states available for their reactions.[35] However, a non-Curtin-Hammett situation can exist for reactions of this type. As exemplified by the pair **62D**−**63**, the energies of the transition states for interconversion of the zwitterionic biradicals can be higher than those for their reactions. In these cases, products derived by reactions at the cation radical sites of the lowest-energy zwitterionic biradicals will dominate.

The results of continuing studies of these processes should lead to a more refined picture of how the energies and reaction rates of zwitterionic biradicals contribute in governing the chemical and quantum yields of SET-photochemical reactions of acceptor−polydonor systems.

Experimental Section

General. All reactions were run under a nitrogen atmosphere. Unless otherwise noted, all reagents were obtained from commercial sources and used without further purification. All compounds were isolated as oils and shown to be >90% pure by ^{1}H and/or ^{13}C NMR, unless otherwise noted. ^{1}H and ^{13}C NMR spectra were recorded on $CDCl_3$ solutions unless otherwise specified and chemical shifts are reported in parts per million (ppm) relative to residual $CHCl_3$ at 7.24 ppm (for ^{1}H NMR) and 77.0 ppm (for ^{13}C NMR). ^{13}C NMR resonance assignments were aided by the use of the DEPT technique to determine numbers of attached hydrogens. Mass spectra were recorded by using electron impact ionization (EI) or fast atomic bombardment (FAB) techniques. Infrared absorption bands are recorded in units of cm^{-1}. Procedures for preparation of the substrates **6**−**13** used for synthesis of the polydonor-linked phthalimides and naphthalimides are given in Supporting Information.

Substrate Synthesis. Phthalimide 14. A solution of alcohol **6** (4.51 g, 16 mmol), phthalimide (2.82 g, 19.2 mmol), triphenylphosphine (5.03 g, 19.2 mmol), and diethyl azodicarboxylate (3.34 g, 19.2 mmol) in THF (80 mL) was stirred for 17 h at 25 °C and filtered through Celite. The filtrate was concentrated in vacuo to give a residue which was subjected to column chromatography (silica gel, 4:1 hexanes−EtAc) to give 2.54 g of phthalimide **14** (74%). ^{1}H NMR 0.11 (s, 9H), 2.30 (s, 3H), 2.56 (t, 2H, J = 6.8 Hz), 2.61 (s, 2H), 2.68 (t, J = 6.5 Hz), 2.74 (s, 3H), 3.23 (t, 3H, J = 6.8 Hz), 3.77 (t, 2H, J = 6.5 Hz), 7.68−7.81 (m, 4H); ^{13}CNMR −1.7, 35.7, 36.1, 38.1, 41.9, 47.6, 55.2 and 55.6, 123.2 and 134.0, 168.1; UV (MeOH), max 293 nm (1600); MS (FAB), *m*/*z* (rel intensity) 412 (100), 217 (45), 174 (20); HRMS(FAB) *m*/*z* 412.1721 ($C_{18}H_{29}N_3O_4SSi$ requires 412.1726).

Phthalimide 15. A solution of alcohol **7** (1.30 g, 4.6 mmol), phthalimide (0.67 g, 4.6 mmol), triphenylphosphine (0.80 g, 4.6 mmol and diethyl azodicarboxylate (0.79 g, 4.6 mmol) in THF (80 mL) was stirred for 17 h at 25 °C and filtered through Celite. The filtrate was concentrated in vacuo to give a residue which was subjected to column chromatography (silica gel, 2:1 hexanes−EtAc) to give of 1.71 g (90%) of phthalimide **15**. ^{1}H NMR 0.12 (s, 9H), 2.69 (s, 2H), 2.80−2.86 (m, 4H), 2.68 (t, 2H, J = 6.5 Hz), 2.86 (s, 3H), 3.35 (t, 3H, J = 6.8 Hz), 3.89 (t, 2H, J = 6.5 Hz), 7.71−7.84 (m, 4H); ^{13}C NMR −1.8, 36.0, 29.3, 29.8, 36.7, 38.8 and 49.7, 123.3, 131.8 and 134.0, 168.0; IR 1691; UV (MeOH) max 293 (1910); MS (FAB), *m*/*z* (rel intensity) 415 (12), 234 (60), 206 (100), 174 (80); HRMS (FAB) *m*/*z* 415.1183 ($C_{17}H_{26}N_2O_4S_2Si$ requires 415.1182).

Phthalimide 16. A solution of potassium phthalimide (0.97 g, 5.25 mmol) and iodide **8** (1.97 g, 5.25 mmol) in 50 mL of DMF was stirred for 8 h at 80 °C, cooled, dried, and concentrated in vacuo to afford a residue which was subjected to column chromatography (silica gel, 1:1:3 EtAc−CH_2Cl_2−hexane) to yield 0.98 g (47%) of phthalimide **16**; mp 102−103 °C; ^{1}H NMR 0.06 (s, 9H), 2.67 (s, 2H), 2.78 (s, 3H), 3.38 (t, 2H, J = 5.3 Hz), 3.60 (t, 2H, J = 5.5 Hz), 3.71 (t, 2H, J = 5.5 Hz), 3.88 (t, 2H, J = 5.0 Hz), 7.71−7.74 (m, 2H), 7.82−7.86 (m, 2H); ^{13}C NMR -1.9, 36.3, 37.3, 37.8, 48.6, 67.7, 67.8, 123.2, 131.9, 134.0, 168.0, 168.5; MS (FAB) *m*/*z* (re. intensity) 399 (81), 383 (23), 321 (37), 247(28), 208(50); HRMS (FAB), *m*/*z* 399.1390 ($C_{17}H_{27}N_2O_2S_1Si$ requires 399.1410).

Phthalimide 17. A solution of potassium phthalimide (972 mg, 5.25 mmoL) and methansulfonate **9** (1.97 g, 5.25 mmol) in 50 mL of DMF was stirred for 8h at 80 °C, cooled, dried, and concentrated in vacuo to afford a residue which was subjected to column chromatography (silica gel, 1:1:3 EtAc−CH_2Cl_2−hexane) yielding 3.42 g (63%) of phthalimide **17**; mp 184−185 °C; ^{1}H NMR (1:2 rotamer mixture), rotamer A −0.01 (s, 9H), 1.98 (s, 3H), 2.71 (s, 2H), 3.36 (t, 2H, J = 5.5 Hz), 3.52 (t, 2H, J = 5.6 Hz), 3.63(t, 2H, J = 5.2 Hz), 3.84 (t, 2H, J = 5.2 Hz), 7.71−7.74 (m, 2H), 7.82−7.86 (m, 2H); rotamer B 0.01 (s, 9H), 1.91 (s, 3H), 2.83 (s, 2H), 3.36 (t, 2H, J = 5.5 Hz), 3.52 (t, 2H, J = 5.6 Hz), 3.63 (t, 2H, J = 5.2 Hz), 3.84(t, 2H, J = 5.2 Hz), 7.71−7.74 (m, 2H), 7.82−7.86 (m, 2H); ^{13}C NMR of rotamer A −1.3, 21.0, 37.1, 38.4, 50.5, 67.9, 68.0, 123.2, 131.9, 134.0, 168.0, 169.5; rotamer B −1.8, 21.7, 37.4, 41.5, 47.3, 67.9, 68.0, 123.2, 131.9, 134.0, 168.0, 169.5; MS (FAB) *m*/*z* (rel intensity) 363 (38), 347 (50), 172 (100); HRMS (FAB) *m*/*z* 363.1747 ($C_{18}H_{27}N_2O_{24}Si_1$ requires 363.1740).

Phthalimide 18. A solution of potassium phthalimide (4.91 mg, 2.65 mmoL) and methanesulfonate **10** (1.00 g, 2.65 mmol) in 60 mL of DMF was stirred for 8 h at 80 °C, cooled, dried, and concentrated in vacuo to afford a residue which was subjected to column chromatography (silica gel, 1:1:3 EtAc−CH_2Cl_2−hexane) yielding 0.55 g (21%) of phthalimide **18**; mp 146−147 °C; ^{1}H NMR 0.07 (s, 9H), 2.67 (s, 2H), 2.82 (s, 3H), 3.37 (t, 2H, J = 5.0 Hz), 3.51−3.57 (m, 6H), 3.67 (m, 2H, J = 5.5 Hz), 3.85 (m, 2H, J = 5.4 Hz); ^{13}C NMR −3.0, 31.0, 32.6, 37.5, 37.7, 38.7, 61.7, 68.4, 72.1, 77.2, 123.3, 134.0, 132.0, 168.5; MS (FAB), *m*/*z* (rel intensity) 443 (65), 427 (15), 339 (20), 363 (23), 319 (7), 208 (70), 174 (100); HRMS (FAB), *m*/*z* 443.1676 ($C_{19}H_{31}N_2O_6S_1Si$ requires 443.1672).

Phthalimide 19. A solution of potassium phthalimide (1.85 g, 10 mmoL) and iodide **11** (3.35 g, 10 mmol) in 60 mL of DMF was stirred for 8 h at 80 °C, cooled, dried, and concentrated in vacuo to afford a residue which was subjected to column chromatography (silica gel, 1:1 EtAc−hexane) yielding 2.96 g (90%) of the ester intermediate. ^{1}H

(35) This is analogous to the Winstein-Holness treatment of the dependence of reaction rates on the population and reactivity of rapidly equilibrating species found in Winstein, S.; Holness, N. J. *J. Am. Chem. Soc.* **1955**, *77*, 5562.

NMR 1.22 (t, 3H, $J = 6.4$ Hz), 2.88 (s, 3H), 3.50 (t, 2H, $J = 5.4$ Hz), 3.79 (t, 2H, $J = 5.8$ Hz), 4.16 (q, 2H, $J = 7.4$ Hz), 4.18 (s, 2H), 7.60−7.64 (m, 2H), 7.74−7.78 (m, 2H); ^{13}C NMR 12.4, 33.2, 38.0, 43.5, 45.7, 59.9, 121.6, 132.3, 130.3, 166.6, 168.0; MS (FAB) *m/z* (rel intensity) 355 (54), 281 (55), 174 (34), 154 (100), 136 (80); HRMS (FAB) *m/z* 355.0977 ($C_{15}H_{19}O_6N_2S_1$, requires 355.0964).

A solution of the ester (1.30 g, 4.5 mmol) and 35% HCl (3 mL) in 15 mL of THF was stirred for 24 h at 60−70 °C, cooled, dried, and concentrated in vacuo to afford a residue which was subjected to crystallization ($CHCl_3$−MeOH) yielding 1.06 g (90%) of phthalimide **19**; mp 202−204 °C; ^{1}H NMR (d_6-acetone) 2.93 (s, 3H), 3.60 (t, 2H, $J = 5.4$ Hz), 4.25 (s, 2H), 7.83 (s, 4H); ^{13}C NMR 32.5, 36.2, 42.6, 44.4, 120.3, 131.4, 129.9, 165.4, 167.8; MS (FAB) *m/z* (rel intensity) 327 (85), 281 (47), 155 (49), 119 (96), 103 (50); HRMS (FAB), *m/z* 327.0659 ($C_{13}H_{15}O_6N_2S_1$, requires 327.0651).

Phthalimide 20. A solution of potassium phthalimide (1.75 g, 11.0 mmoL) and iodide **12** (2.8 g, 7.38 mmol) in 50 mL of DMF was stirred for 8 h at 80 °C, cooled, dried, and concentrated in vacuo to afford a residue which was subjected to column chromatography (silica gel, 1:1:3 EtAc−CH_2Cl_2−hexane) yielding 1.45 g (51%) of the intermediate ester. ^{1}H NMR 1.25 (t, 3H, $J = 7.2$ Hz), 2.96 (s, 3H), 3.39 (t, 2H, $J = 5.0$ Hz), 3.59−3.65 (m, 4H), 3.85 (t, 2H, $J = 4.8$ Hz), 4.09−4.21 (m, 4H); ^{13}C NMR 14.1, 37.3, 39.8, 47.8, 49.6, 61.3, 68.0, 70.4, 123.3, 134.0, 134.0, 168.5, 170.2; MS (FAB) *m/z* (rel intensity) 399 (46), 391 (5), 325 (10), 289 (90), 260 (32), 216 (30), 208 (100); HRMS (FAB), *m/z* 399.1229 ($C_{17}H_{23}N_2O_7S_1$ requires 399.1226).

A solution of the ester (0.3 g, 0.75 mmol) and 35% HCl (0.13 mL, 1.55 mmol) in 30 mL of THF was stirred for 48 h at 50 °C, dried, and concentrated in vacuo to afford a residue which was subjected to crystallization ($CHCl_3$−Et_2O) yielding 0.10 g (37%) of phthalimide **20**; mp 164−165 °C ($CHCl_3$−Et_2O); ^{1}H NMR (d_6-DMSO) 2.89 (s, 3H), 3.28(t, 2H, $J = 5.0$ Hz), 3.49 (t, 2H, $J = 4.8$ Hz), 3.68 (t, 2H, $J = 4.8$ Hz), 3.71 (t, 2H, $J = 4.8$ Hz), 3.88 (s, 2H) 7.60 (s, 4H); ^{13}C NMR (d_6-DMSO) 36.1, 40.6, 46.1, 47.7, 66.1, 67.0, 122.0, 130.5, 133.4, 166.8, 166.9; MS (FAB), *m/z* (rel intensity) 371 (100), 325 (30), 291 (9), 247 (11), 192 (26); HRMS (FAB) *m/z* 371.0953 ($C_{15}H_{19}N_2O_7S_1$ requires 371.0913).

Phthalimide 21. A solution of phthalimide (0.71 g, 4.18 mmol), triphenylphosphine (1.26 g, 4.81 mmol), alcohol **13** (1.36 g, 4.18 mmol) and diisopropyl azodicarboxylate (0.95 mL, 4.18 mmol) in 60 mL was stirred for 20 h at room temperature, and concentrated in vacuao. The residue was subjected to column chromatography (silica gel, 1:1:1 EtAc−CH_2Cl_2−hexane) yielding 0.8 g (41%) the intermediate ester. ^{1}HNMR 1.24 (t, $J = 6.9$ Hz), 2.25 (s, 3H), 2.57−2.62 (m, 4H), 2.93 (s, 3H), 3.24 (t, 2H, $J = 3.3$ Hz), 3.71 (t, 2H, $J = 2.1$ Hz), 4.07 (s, 2H), 4.14 (q, 2H, $J = 6.8$ Hz), 7.66−7.69 (m, 2H), 7.76−7.78 (m, 2H); ^{13}C NMR 14.1, 35.5, 39.6, 42.0, 45.5, 48.7, 55.3, 56.3, 61.3, 123.1, 133.9, 132.0, 168.2, 169.8; MS (FAB), *m/z* (rel intensity) 412 (84), 410 (53), 251 (31), 217 (100), 174 (63); HRMS (FAB) *m/z* 412.1553 ($C_{18}H_{26}O_6N_3S_1$, requires 412.1542).

A solution of the ester (0.7 g, 1.7 mmol) and 35% HCl (3 mL) in 15 mL of THF was stirred for 24 h at 80 °C, cooled dried, and concentrated in vacuo to afford a residue which was subjected to crystallization ($CHCl_3$−Et_2O) yielding 390 mg (60%) of phthalimide **21**; mp 205−208 °C ($CHCl_3$-Et_2O); ^{1}H NMR (d_6-DMSO) 2.84 (s, 3H), 3.05 (s, 3H), 3.34−3.37 (m, 4H), 3.58 (m, 2H), 3.95 (m, 2H), 4.04 (s, 2H,), 7.84−7.85 (s, 4H); ^{13}C NMR; 31.5, 37.1, 39.0, 41.4, 47.8, 51.8, 52.1, 122.1, 133.4, 130.9, 166.8, 169.9; MS (FAB), *m/z* (rel intensity) 384 (100), 326 (1), 306 (2), 254 (5), 217 (10), 174 (11); HRMS (FAB) *m/z* 384.1217($C_{16}H_{22}O_6N_3S_1$, requires 384.1229).

Naphthalimide 27. A solution of methansulfonate **22**[17] (0.62 g, 2 mmol), potassium 2,3-naphthalenedicarboximide (0.24 g, 1 mmol) and hexadecyltributylphosphonium bromide (0.10 g, 0.2 mmol) in DMF (10 mL) was stirred for 2 h at 80 °C and poured into ice−water. The solid was filtered and subjected to column chromatography (silica gel, 10:1 CH_2Cl_2−EtAc) to give the **27** (0.34 g, 83%); mp 231−232 °C (CH_2Cl_2−hexane); ^{1}H NMR 0.17 (s, 9H), 2.77 (s, 3H), 2.82 (s, 2H), 3.52 (t, 2H, $J = 6.3$ Hz), 3.96 (t, 2H, $J = 6.2$ Hz), 7.66−7.69 (m, 2H), 8.02−8.05 (m, 2H), 8.33 (s, 2H); ^{13}C NMR −1.6, 36.2, 36.6, 39.1, 47.6, 124.8, 127.7, 129.2, 130.3, 135.5, 167.8; IR 1716; UV (MeCN) max 256 nm (63000); MS (FAB) *m/z* 405 ($M^+ + 1$), 389, 325, 253, 224, 210, 116, 73; HRMS (FAB) *m/z* 405.1315 ($C_{19}H_{25}N_2O_4SSi$ requires 405.1304).

Naphthalimide 28. A solution of methansulfonate **23**[18] (0.6 g, 1.4 mmol), potassium 2.3-naphthalenedicarboximide (0.24 g, 1 mmol), and hexadecyltributylphosphonium bromide (0.1 g, 0.2 mmol) in DMF (10 mL) was stirred for 2 h at 80 °C and poured into ice−water. The solid was filtered and subjected to column chromatography (silica gel, 2:2:1 EtAc−CH_2Cl_2−hexane) to afford the **28** (0.4 g 74%); mp 195−196 °C (CH_2Cl_2−hexane); ^{1}H NMR 0.14 (s, 9H), 2.69 (s, 2H), 2.79 (s, 3H), 2.91 (s, 3H), 3.44−3.58 (m, 6H), 3.97 (t, 2H, $J = 5.8$ Hz), 7.65−7.69 (m, 2H), 8.01−8.04 (m, 2H), 8.32 (s, 2H). ^{13}C NMR −1.8, 34.2, 37.0, 37.7, 40.8, 47.1, 48.2, 50.1, 124.9, 127.7, 129.2, 130.3, 135.5, 168.0; IR: 1708; UV (MeCN) max 256 nm (58000); MS (FAB) *m/z* 526 ($M^+ + 1$), 448, 374, 253, 224, 194; HRMS (FAB) *m/z* 526.1498 ($C_{22}H_{31}N_3O_6S_2Si$ requires 526.1502).

Naphthalimide 29. A solution of potassium naphthalenedicarboximide (0.36 g, 1.5 mmol), methansulfonate **8** (0.7 g, 2 mmol), and hexadecyltributylphosphonium bromide (0.2 g, 0.4 mmol) in 10 mL DMF was stirred for 2 h at 80 °C and poured into ice water. The solid was filtered and subjected to column chromatography (silica gel, 1:1 EtAc−hexane) to afford **29** (0.55 g, 80%); mp 133−134 °C (CH_2Cl_2−hexane); ^{1}H NMR 0.05 (s, 9H), 2.67 (s, 2H), 2.77 (s, 3H), 3.39 (t, 2H, $J = 5.4$ Hz), 3.62 (t, 2H, $J = 5.4$ Hz), 3.76 (t, 2H, 5.6 Hz), 3.95 (t, 2H, $J = 5.6$ Hz), 7.67−7.71 (m, 2H), 8.03−8.07 (m, 2H), 8.32 (s, 2H). ^{13}C NMR −1.8, 36.4, 37.6, 38.0, 48.8, 67.8, 67.9, 124.7, 127.7, 129.3, 130.3, 135.4, 167.9. IR: 1740; UV (MeCN) max 258 nm (69000); MS (FAB) *m/z* 449 ($M^+ + 1$), 433, 371, 297, 224, 208, 137, 116, 73; HRMS (FAB) *m/z* 449.1578 ($C_{21}H_{29}N_2O_5SSi$ requires 449.1566).

Naphthalimide 30. A solution of 2,3-naphthalenedicarboximide (0.5 g, 2.5 mmol), triphenylphosphine (0.73 g. 2.8 mmol), alcohol **24**[16] (0.45 g, 2.8 mmol), and diethyl azodicarboxylate (0.49 g, 2.8 mmol) in THF (35 mL) was stirred for 12 h at 25°C and poured into ice water. The resulting precipitate was separated by filtration and subjected to column chromatography (silica gel, 1:1 EtAc−hexane) to give naphthalimide **30** (0.78 g, 90%) mp 119−120 °C (hexane); ^{1}H NMR −0.03 (s, 9H), 1.95 (s, 2H), 2.28 (s, 3H), 2.62 (t, 2H, $J = 6.7$ Hz), 3.84 (t, 2H, 6.6 Hz), 7.65−7.70 (m, 2H), 8.00−8.05 (m, 2H), 8.30 (s, 2H); ^{13}C NMR −1.5, 36.3, 46.1, 49.8, 58.9, 124.4, 128.1, 129.0, 130.3, 135.4, 168.1; IR: 1744; UV (MeCN) max 256 nm (67000); MS (FAB) *m/z* 341 ($M^+ + 1$), 267, 224, 180, 130; HRMS (FAB) *m/z* 341.1689 ($C_{19}H_{25}N_2O_2Si$ requires 341.1685).

Naphthalimide 31. A solution of 2,3-naphthalenedicarboximide (1.97 g, 10 mmol), alcohol **6** (3.6 g, 12.8 mmol), and triphenylphosphine (3.4 g, 13.0 mmol),, and diethyl azodicarboxylate (2.3 g, 13.2 mmol) in THF (55 mL) was stirred overnight at room temperature and poured into ice water. The solid was filtered and subjected to column chromatography (silica gel, 2:2:1 EtAc−CH_2Cl_2−hexane) to give **31** (3.1 g, 67.1%); mp 141−142 °C (EtAc−hexane); ^{1}H NMR 0.06 (s, 9H), 2.33 (s, 3H), 2.56−2.61 (m, 4H), 2.71−2.76 (m, 5H), 3.26 (t, 2H, $J = 6.7$ Hz), 3.85 (t, 2H, $J = 6.5$ Hz), 7.67−7.70 (m, 2H), 8.02−8.06 (m, 2H), 8.30 (s, 2H); ^{13}C NMR −1.7, 36.0, 36.1, 38.0, 41.9, 47.6, 55.2, 55.6, 124.6, 127.8, 129.2, 130.3, 135.4, 168.0; IR 1704; UV (MeCN) max 256 nm (70000); MS (FAB) *m/z* 462 ($M^+ + 1$), 382, 267, 224, 116, 73; HRMS (FAB) *m/z* 462.1905 ($C_{22}H_{32}N_3O_4SSi$ requires 461.1883)

Naphthalimide 32. To a solution of 2.3-naphthalenedicarboximide (503 mg, 2.55 mmoL), in DMF (40 mL) was added NaH (2.50 g, 16.7 mmoL) portionwise over a 2 h period with stirring. To this solution was added methansulfonate **10** (1.0 g, 2.55 mmol) in 10 mL DMF dropwise. After stirring for 12h at 80 °C, the solution was dried and concentrated in vacuo to afford a residue which was subjected to column

chromatography (silica gel, 1:1:1 EtAc−CH_2Cl_2−hexane) yielding 0.59 g (52%) of naphthalimide **32**; mp 156−157 °C; ^{1}H NMR 0.07 (s, 9H), 2.67 (s, 2H), 2.83 (s, 3H), 3.37 (t, 2H, J = 5.0 Hz), 3.53−3.61 (m, 6H), 3.74 (t, 2H, J = 5.6 Hz), 3.93 (t, 2H, J = 5.8 Hz), 7.65−7.70 (m, 2H), 8.01−8.05 (m, 2H), 8.30 (s, 2H); ^{13}C NMR -1.8, 36.2, 37.4, 48.7,, 67.8, 70.0, 70.1, 124.7, 127.5, 130.2, 129.2, 135.3, 167.6;

Naphthalimide 33. A solution of potassium 2,3-naphthalenedicarboximide (1.00 g, 5.07 mmol) and methansulfonate **9** (1.58 g, 5.07 mmol) in 60 mL DMF was stirred for 8 h at 80 °C, cooled, dried, and concentrated in vacuo to afford a residue which was subjected to column chromatography (silica gel, 1:1:3 EtAc−CH_2Cl_2−hexane) yielding 2.09 g (60%) of naphthalimide **33**. ^{1}H NMR (1:2 mixture of two rotamers) rotamer A −0.02 (s, 9H), 2.04 (s, 3H), 2.88 (s, 2H), 3.39 (t, 2H, J = 5.5 Hz), 3.57 (t, 2H, J = 5.6 Hz), 3.72 (t, 2H, J = 5.2 Hz), 3.93 (t, 2H, J = 5.2 Hz), 7.66−7.71 (m, 2H), 8.02−8.07 (m, 2H), 8.33 (s, 2H); ^{1}H NMR of rotamer 0.05 (s, 9H), 1.95 (s, 3H), 2.76 (s, 2H), 3.39 (t, 2H, J = 5.5 Hz), 3.57 (t, 2H, J = 5.6 Hz), 3.72 (t, 2H, J = 5.2 Hz), 3.95 (t, 2H, J = 5.2 Hz), 7.66−7.71 (m, 2H), 8.02−8.07 (m, 2H), 8.33 (s, 2H); ^{13}C NMR of rotamer A −1.3, 21.2, 37.4, 38.5, 50.5, 67.9, 68.0, 124.6, 127.6, 130.1, 129.1, 135.0, 167.9, 169.7; ^{13}C NMR of rotamer B −1.7, 21.9, 37.7, 41.5, 47.3, 67.9, 68.0, 124.6, 127.6, 130.1, 129.1, 135.0, 167.9, 169.7; MS (FAB) *m*/*z* 413 (M^+ + 1), 397, 371, 224, 172; HRMS (FAB) *m*/*z* 413.1904 ($C_{22}H_{29}N_2O_4Si$ requires 413.1897)

Naphthalimide 34. To a solution of 2.3-naphthalenedicarboximide (0.5 g, 2.5 mmol), in DMF (40 mL) was added NaH (0.12 g, 3 mmol) in portions over a 2 h period. To this solution was iodide **11** (0.8 g, 2.5 mmol) in 10 mL DMF. After stirring for 8 h at 80 °C, the solution was cooled, dried, and concentrated in vacuo to afford a residue which was subjected to column chromatography (silica gel, 1:1:1 EtAc−$CHCl_3$−hexane) yielding 0.7 g (70%) of the intermediate ester. ^{1}H NMR 1.29 (t, 3H, J = 6.4 Hz), 2.94 (s, 3H), 3.60 (t, 2H, J = 5.4 Hz), 3.93 (t, 2H, J = 5.2 Hz), 4.21 (q, 2H, J = 7.4 Hz), 4.27 (s, 2H), 7.64−7.69 (m, 2H), 8.00−8.04 (m, 2H), 8.33 (s, 2H); ^{13}C NMR 12.5, 33.4, 38.1, 43.5, 45.8, 60.0, 123.2, 127.4, 128.6, 126.1, 133.8, 166.4, 168.1; MS (FAB) *m*/*z* (rel intensity) 405 (100), 391 (60), 149 (100); HRMS (FAB) *m*/*z* 405.1106 ($C_{19}H_{21}O_6N_2S_1$, requires 405.1120).

A solution of this ester (700 mg, 1.73 mmol) and 35% HCl (3 mL) in 20 mL of THF was stirred for 24 h at 60−70 °C, cooled, dried, and concentrated in vacuo to afford a residue which was subjected to crystallization ($CHCl_3$−MeOH) yielding 520 mg (80%) of naphthalimide **34**; mp 200−203 °C; MeOH−$CHCl_3$); ^{1}H NMR (d_6-DMSO) 2.97 (s, 3H), 3.45 (m, 2H,), 3.55 (s, 2H), 3.73 (t, 2H, J = 5.2 Hz), 7.70−7.75 (m, 2H), 8.19−8.24 (m, 2H), 8.44 (s, 2H); ^{13}C NMR (d_6-DMSO**)** 34.5, 38.9, 43.5, 49.3, 123.2 128.1, 129.1, 126.7, 133.9, 165.3, 169.4; MS (FAB) *m*/*z* (rel intensity) 377 (0.5), 329 (28), 177(40), 135 (100); HRMS (FAB) *m*/*z* 377.0826 ($C_{17}H_{17}O_6N_2S_1$, requires 377.0807).

Naphthalimide 35. A solution of 2,3-naphthalenedicarboximide (2.1 g, 6.21 mmol), triphenylphosphine (1.63 g, 6.21 mmol), alcohol **26**[16] (1 g, 6.21 mmol), and diethyl azodicarboxylate (1.08 g, 6.21 mmol) in 60 mL of THF was stirred for 5 h at room temperature, and concentrated in vacuo, giving a residue which was subjected to column chromatography (silica gel, 1:1 EtAc−hexane) yielding 970 mg (46%) of the intermediate ester. ^{1}H NMR 1.24 (t, 3H, J = 0.8 Hz), 2.48 (s, 3H), 2.92 (t, 2H, J = 6.6 Hz), 3.35 (s, 2H), 3.87 (t, 2H, J = 6.2 Hz), 4.11 (q, 2H, J = 7.0 Hz) 7.64−7.69 (m, 2H), 8.00−8.05 (m, 2H), 8.30 (s, 2H); ^{13}C NMR 14.2, 35.9, 41.9, 54.0, 58.0, 60.4, 124.5, 129.0, 130.2, 127.9, 135.4, 168.0, 170.7; MS (FAB) *m*/*z* (rel intensity) 341 (100), 339 (30), 267 (30), 224 (87), 130 (28); HRMS (FAB) *m*/*z* 341.1513 ($C_{19}H_{12}O_4N_2$, requires 341.1501).

A solution of this ester (1.17 g, 3.45 mmol) and 35% HCl (3 mL) in 25 mL of THF was stirred for 24 h at 50−70 °C, cooled, dried and concentrated in vacuo to afford a residue which was subjected to crystallization ($CHCl_3$−MeOH) yielding 683 mg (73%) of naphthalimide **35**; mp 258−260 °C; MeOH−$CHCl_3$); ^{1}H NMR (d_6-DMSO) 2.92 (s, 3H), 3.70 (m, 2H), 4.03 (m, 2H), 4.17 (s, 2H), 7.75−7.79 (m, 2H), 8.24−8.29 (m, 2H), 8.54 (s, 2H); ^{13}C NMR (d_6-DMSO**)** 31.8, 39.9, 52.4, 53.9, 123.5, 128.4, 129.3, 126.7, 133.9, 166.4, 166.6; MS (FAB) *m*/*z* (rel intensity) 313 (100), 257 (20), 224 (51), 175 (11); HRMS (FAB) *m*/*z* 313.1188 ($C_{17}H_{17}O_4N_2$, requires 313.1188).

Naphthalimide 36. A solution of 2.3-naphthalenedicarboximide (1.91 g, 9.7 mmol), triphenylphosphine (2.54 g, 9.7 mmol), alcohol **13** (2.75 g, 9.7 mmol), and diisopropyl azodicarboxylate (1.91 mL, 9.7 mmol) in 40 mL of THF was stirred overnight at room temperature and concentrated in vacuo, and the residue was subjected to column chromatography (silica gel, 1:1:1 EtAc−$CHCl_3$−hexane) yielding 0.8 g (41%) of the intermediate ester. ^{1}H NMR 1.20 (t, 3H, J = 4.8 Hz), 2.28 (s, 3H), 2.60 (t, 2H), 2.68 (t, 4H, J = 4.4 Hz) 2.94 (s, 3H), 3.28 (t, 2H, J = 4.4 Hz), 3.81 (t, 2H, J = 4.2 Hz), 4.09 (s, 2H), 4.12 (q, 2H, J = 4.0 Hz), 7.65−7.68 (m, 2H), 8.14−8.17 (m, 2H), 8.41 (s, 2H); ^{13}C NMR 14.1, 35.9, 39.7, 44.0, 45.7, 48.8, 55.3, 56.4, 61.3, 124.5, 129.1, 130.2, 127.8, 130.2, 167.9, 169.9; MS (FAB) *m*/*z* (rel intensity) 462 (100), 460 (10), 282 (5), 267 (33), 251 (10), 224 (24); HRMS (FAB) *m*/*z* 462.1686 ($C_{22}H_{28}O_6N_3S_1$, requires 462.1699).

A solution of the ester (1 g, 2.1 mmol) and 35% HCl (3 mL) in 25 mL of H_2O was stirred for 24 h at 50−60°C, cooled, dried, and concentrated in vacuo to afford a residue which was subjected to crystallization ($CHCl_3$−MeOH) yielding 750 mg (80%) of phthalimide **36**; mp 200−203 °C; MeOH−$CHCl_3$); ^{1}H NMR (d_6-DMSO) 2.78 (s, 3H), 2.95 (s, 3H), 3.24−3.48 (m, 4H), 3.54 (m, 2H), 3.92 (m, 2H), 3.96 (s, 2H), 7.65−7.68 (m, 2H), 8.14−8.17 (m, 2H), 8.41 (s, 2H); ^{13}C NMR (d_6-DMSO) 31.6, 37.2, 39.0, 41.7, 47.8, 51.9, 52.1, 123.4, 128.4, 129.2, 126.2, 133.8, 166.6, 170.1; MS (FAB) *m*/*z* (rel intensity) 434 (100), 310 (5), 267 (14), 224 (28), 119 (10); HRMS (FAB) *m*/*z* 434.1399 ($C_{20}H_{24}O_6N_3S_1$, requires 434.1386).

Preparative Photochemistry. Preparative photochemical reactions of the phthalimide and naphthalimide substrates in the specified solvent were conducted by using an apparatus consisting of a 450-W medium-pressure mercury lamp surrounded by a Pyrex glass filter in a quartz immersion well. The irradiated solutions were maintained at 17 °C under a N_2 atmosphere. In each case, photoreaction progress was monitored by using UV spectroscopy, and irradiation was terminated when ca. 90% of the substrate was consumed. In each case, concentration of the photolysate was followed by silica gel column chromatography to give the photoproduct(s) unless otherwise noted.

Conversion of 14 to 46−47. A solution of **14** (118 mg, 0.28 mmol) and 0.02 M $HClO_4$ in 250 mL of MeOH was irradiated for 2.5 h. Chromatographic separation (silica gel, 1:1 EtAc−hexane) gave 85 mg (88%) of **46** and 12 mg of **47** (12%).

46: ^{1}H NMR 2.36 (s, 3H), 2.56 (s, 3H), 2.58−2.62 (m, 2H), 2.74−2.82 (m, 2H), 3.22 (s, 1H), 3.37−3.41 (m, 2H), 3.74 and 4.17 (abq, 2H, J = 14.0), 3.81−3.87 (m, 2H), 7.32−7.59 (m, 4H); ^{13}C NMR 36.6, 46.5, 39.5, 49.9, 56.0, 56.9, 58.0, 121.3, 123.2, 129.3, 132.1, 129.8, 145.0, 167.1; IR 3100−3550, 1691; MS (FAB), *m*/*z* (rel intensity) 340 (100), 322 (25), 260 (20), 157 (70); HRMS (FAB) *m*/*z* 340.1324 ($C_{15}H_{21}N_3O_4S$ requires 340.1331).

47: ^{1}H NMR 2.06 (s, 3H), 2.42 (s, 3H), 2.73 (s, 3H), 2.46−2.56, 2.75−2.81, 2.92−3.00, 3.18−3.24 and 3.77−3.79 (m, 8H), 4.84 and 4.45 (abq, 2H, J = 14.7 Hz), 7.51−7.81 (m, 4H); ^{13}C NMR 39.2, 46.7 and 49.7, 41.2, 43.6, 49.7, 53.9, 58.8, 123.3, 124.1, 130.3, 132.3, 132.9, 142.1, 168.4; IR 3200−3600, 1695; MS (FAB), *m*/*z* (rel intensity) 354 (100), 322 (30), 274 (25); HRMS (FAB) *m*/*z* 354.1488 ($C_{16}H_{23}N_3O_4S$ requires 354.1488).

Conversion of 14 to 43−45. A solution of **14** (538 mg, 1.31 mmol) in 250 mL of MeOH was irradiated for 4 h. Column chromatography (silica gel, 1:3 EtAc−hexane) followed by HPLC (4:1 MeCN−water) gave 128 mg of **43** (52%), 55 mg of **44** (22%), and 48 mg of **45** (20%).

43: ^{1}H NMR 0.043 (s, 9H), 2.11 (s, 1H, OH), 2.34 (s, 3H), 2.59 and 2.53 (abq, 2H, J = 15.0 Hz), 2.48−2.81 (m, 4H), 3.14−3.18, 3.28−3.31 and 4.10−4.13 (m, 4H), 5.69 (s, 1H), 7.41−7.68 (m, 4H); ^{13}C NMR −1.9, 34.9, 42.0, 39.3, 40.0, 47.9, 55.9, 57.3, 82.5, 123.0, 123.1, 129.2, 132.2, 131.1, 144.3, 167.5; IR 3100−3600, 1691; MS (FAB)

m/*z* (rel intensity) 414 (100), 396 (90); HRMS (FAB) *m*/*z* 414.1897 ($C_{16}H_{31}N_3O_4SSi$ requires 414.1896).

44: ^{1}H NMR 0.11 (s, 9H), 2.62 and 2.66 (abq, 2H, J = 15.3 Hz), 2.71−2.78, 2.83−2.87, 3.04−3.07, 3.11−3.17, 3,21−3.24, and 4.29−4.33 (m, 8H), 5.74 (s, 1H), 7.43−7.74 (m, 4H);^{13}C NMR −1.6, 34.6, 40.7, 42.2, 47.6, 48.8, 50.1, 82.6, 123.0, 123.3, 129.3, 132.2, 131.1, 144.2, 164.0; IR 3100−3520, 1695; MS (FAB) *m*/*z* (rel intensity) 400 (50), 382 (55), 303 (40), 157 (25); HRMS (FAB) *m*/*z* 400.1724 ($C_{17}H_{29}N_3O_4SSi$ requires 400.1726).

45: ^{1}H NMR 0.15 (s, 9H), 2.06−2.16, 2.55−2.69, 2.89−2.91, 3.29−3.91 and 4.15−4.26 (m, 10H), 2.96 (s, 3H), 5.10 (s, 1H), 7.43−7.79 (m, 4H); ^{13}C NMR −1.7, 36.1, 37.6, 46.5, 52.4, 53.9, 63.0, 85.2, 121.9, 123.5, 129.7, 132.1, 128.5, 144.8, 164.9; IR 3150−3600, 1691; MS (FAB), *m*/*z* (rel intensity) 410 (60), 394 (100), 279 (28), 217 (55), 200 (33); HRMS (FAB) *m*/*z* 410.1581 ($C_{18}H_{29}N_3O_4SSi$ requires 410.1570).

Conversion of 15 to 39. A solutions of **15** (306 mg, 0.74 mmol) in 250 mL of MeOH was irradiated for 3 h. Column chromatography (silica gel, 1:1 EtAc−hexane) gave 245 mg (97%) of **39**.^{1}H NMR 2.61−2.67, 2.78−2.86, 3.16−3.22, 3.51−3.57, 3.62−3.65 and 3.90−3.93 (m, 8H), 4.61 and 3.82 (abq, 2H, J = 15.3 Hz), 5.24 (s, 1H), 7.44−7.66 (m, 4H); ^{13}C NMR 31.0, 32.8, 42.4, 44.9, 55.1, 37.3, 88.4, 122.3, 123.4, 130.1, 132.6, 130.7, 145.7, 168.9; IR 3120−3500, 1695; MS (FAB) *m*/*z* (rel intensity) 343 (21), 246 (9), 157 (30); HRMS (FAB) *m*/*z* 343.0775 ($C_{14}H_{18}N_2O_4S_2Si$ requires 343.0786).

Conversion of 16 and 18 to 40 and 42. Independent solutions of **16**, **18** (100 mg and 111 mg, 2.5 mmol) in 150 mL of MeOH were irradiated for 0.5 h each. Column chromatography (silica gel, 1:1:3 EtAc−CH_2Cl_2−hexane) gave 74 and 82 mg (91 and 89%) of the respective products **40** and **42**.

40: (mp 102−103 °C; hexanes−EtAc−$CHCl_3$). ^{1}H NMR 2.47 (s, 3H), 3.32 (t, 2H, J = 4.4 Hz), 3.63−3.78 (m, 4H), 3.92−3.98 (m, 2H, J = 4.8 Hz), 4.14 and 4.42 (abq, 2H, J = 15.5 Hz), 7.52−7.56 (m, 2H), 7.62−7.65 (m, 1H), 7.77 (d, 1H); ^{13}C NMR 37.6, 42.1, 48.5, 53.9, 68.2, 71.1, 88.7, 122.9, 123.4, 130.2, 131.0, 132.5, 145.1, 168.1; MS (FAB) *m*/*z* (rel intensity) 309 (32), 307 (7), 155 (70), 119 (100); HRMS (FAB) *m*/*z* 309.0901 ($C_{14}H_{17}N_2O_4S$ requires 309.0909).

42: (mp 146−147 °C; hexanes−EtAc−$CHCl_3$). ^{1}H NMR (d_6-DMSO) 2.12 (s, 3H), 3.32 (t, 2H, J = 4.4 Hz), 3.63−3.78 (m, 8H), 3.87 (t, 2H, J = 4.8 Hz), 4.05 and 4.42 (abq, 2H, J = 15.5 Hz); ^{13}C NMR (d_6-DMSO) 37.2, 39.5, 45.5, 48.5, 67.5, 67.9, 69.5, 70.2, 89.2, 121.1, 123.6, 128.5, 130.4, 130.6, 145.9, 167.9; *m*/*z* (rel intensity) 371 (75), 353 (20), 274 (100), 157 (40); HRMS (FAB) *m*/*z* 371.1277 ($C_{16}H_{23}N_2O_6S$ requires 371.1277).

Conversion of 17 to 41. A solution of **17** (134 mg, 0.37 mmol) in 150 mL of MeOH was irradiated for 0.5 h. Column chromatography (silica gel, 1:1:3 EtAc−CH_2Cl_2−hexane) gave 100 mg (93%) of product **41**; mp 175−177 °C (hexanes−EtAc−$CHCl_3$); ^{1}H NMR 2.26 (s, 3H), 3.32 (t, 2H, J = 4.4 Hz), 3.63−3.78 (m, 4H), 3.92−3.98 (m, 2H, J = 4.8 Hz), 4.23 (d, 2H, J = 12.6 Hz), 4.82 (d, 2H, J = 14.6 Hz), 7.47−7.56 (m, 2H), 7.56−7.58 (m, 1H), 7.75 (d, 1H); ^{13}C NMR 22.5, 43.1, 48.5, 53.8, 68.6, 69.0, 90.1, 121.6, 123.3, 129.7, 132.5, 132.5, 147.5.

Conversion of 19 to 48. Irradiation of **19** (400 mg, 1.23 mmol) and tetrabutylamonium hydroxide (1.23 mL, 1.0 M CH_3OH) in 200 mL of MeOH followed by column chromatography (silica gel, 1:1 EtAc−hexane) gave 339 mg (98%) of known[17] **48**.

Conversion of 20 to 40. Irradiation of **20** (137 mg, 0.37 mmol) tetrabutylamonium hydroxide (0.37 mL, 1.0 M CH_3OH) in 200 mL of MeOH for 20 min followed by column chromatography (silica gel, 1:1:3 EtAc−CH_2Cl_2−hexane) yielded 110 mg (95%) of product **40**.

Conversion of 27 to 49. A solution of **27** (15 mg, 0.037 mmol) in 150 mL of 1:1 CH_3CN−CH_3OH was irradiated for 0.5 h. The residue obtained from concentration of photolysate was pure **49** (12.3 mg, 100%); mp 261−262 °C (CH_3OH); ^{1}H NMR (d_6-DMSO) 2.83 and 4.20 (two d, 2H, J = 12.5 Hz), 2.85−2.90 (m, 1H), 3.00 (s, 3H), 3.36−3.39 (m, 1H), 3.73−3,75 (m, 1H), 4.11−4.15 (m, 1H), 6.81 (s, 1H), 7.62−7.70 (m, 2H), 8.10 and 8.17 (two d, J = 8.1 Hz), 8.27 (s, 1H), 8.37 (s, 1H). ^{13}C NMR (d_6-DMSO) 35.4, 36.7, 44.5, 53.6, 83.8, 121.8, 123.2, 127.1, 128.1, 128.6, 129.1, 129.5, 133.4, 134.8, 141.2. 163.7. IR: 3600−3200, 1670; MS (FAB) *m*/*z* 333 (M^+ + 1), 315, 253, 235, 205, 177, 152, 133, 103, 89, 73; HRMS (FAB) *m*/*z* 333.0891 ($C_{16}H_{17}N_2O_4S$ requires 333.0909).

Conversion of 28 to 50. A solution of **28** (74 mg, 0.14 mmol) in 150 mL of 1:1 CH_3CN−CH_3OH was irradiated for 0.5 h. The residue obtained by concentration of the photolysate was pure **50** (64 mg, 100%); mp 364−365 °C, MeCN); ^{1}H NMR (d_6-DMSO) 2.60 (s, 3H), 2.89−2.94 (m, 2H), 2.98 (s, 3H), 3.17−3.20 (m, 1H), 3.31−3.36 (m, 1H), 3.45−3.50 (m,1H), 3.75−3.84 (m, 3H), 4.26 and 4.36 (two d, 2H, 14.8 Hz), 6.86 (s,1H), 7.63−7.67 (m, 2H), 8.07−8.09 (m, 2H), 8.16 (d, 1H, J = 8 Hz), 8.35 (s, 1H), ^{13}C NMR (d_6-DMSO) 35.4, 39.5, 40.8, 41.9, 47.3, 49.2(2), 88.3, 122.6, 122.9, 127.0, 128.1, 128.7, 128.8, 129.5, 133.3, 134.8, 141.0, 167.0, IR: 3600−3200, 1668; MS (FAB) *m*/*z* 454 (M^+ + 1), 436, 374, 278, 233, 119; HRMS (FAB) *m*/*z* 454.1103 ($C_{19}H_{24}N_3O_6S_2$ requires 454.1107).

Conversion of 29 to 51. A solution of **29** (350 mg, 0.78 mmol) in 150 mL 1:1 CH_3CN−CH_3OH was irradiated for 1 h. Chromatography (silica gel, 10:1 EtAc−hexane) gave **51** (260 mg, 88%); mp 274−276 °C (EtAc−hexane); ^{1}H NMR 2.95−3.05 (m, 1H), 3.15−3.19 (m, 1H), 3.34 (s, 3H), 3.41−3.45 (m, 2H), 3.59−3.68 (m, 2H), 3.91−3.97 (m, 2H), 4.18 and 4.30 (two d, J = 14.6 Hz), 6.82 (s, 1H), 7.62−7.66 (m, 2H). 8.07−8.09 (m, 2H), 8.17 (d, 1H, J = 8.0 Hz), 8.33 (s, 1H). ^{13}C NMR (d_6-DMSO) 39.0, 40.2, 43.7, 49.9, 67.1, 71.2, 88.8, 122.6, 123.0, 126.9, 128.0, 128.7, 129.1, 129.5, 133.2, 134.7, 141.1, 166.8; IR: 3600−3200, 1659; MS (FAB) *m*/*z* 377 (M^+ + 1), 359, 297, 233, 157, 119; HRMS (FAB) *m*/*z* 377.1186 ($C_{18}H_{21}N_2O_5S$ requires 377.1171).

Conversion of 30 to 54−56. A solution of **30** (380 mg, 1.12 mmol) in 150 mL of 1:1 CH_3CN−CH_3OH was irradiated for 4 h. Chromatography (silca gel 10:1 EtAc−hexane) gave **54** (150 mg, 50%), **55** (50 mg, 17%), and **56** (20 mg, 7%).

54: mp 175−176 °C (EtAc−hexane); ^{1}H NMR 2.01−2.09 (m, 2H), 2.41(s, 3H), 2.88 and 2.91 (two d, 1H, J = 3.6 Hz), 3.35−3.43 (m, 2H), 4.24 and 4.27 (two d, 1H, J = 3.6 Hz), 6.47(s, 1H), 7.53−7.60 (m, 2H), 7.91 and 7.95 (two d, 2H, J = 7.9 Hz), 7.97 (s, 1H), 8.28 (s, 1H). ^{13}C NMR 36.0, 45.7, 53.9, 63.8, 85.0, 121.2, 123.8, 126.7, 127.7, 128.3, 128.9, 129.4, 133.5, 134.9, 140.2. 164.7; IR: 3600−3200, 1691; MS (FAB) *m*/*z* 269 (M^+ + 1), 251, 133, 73; HRMS (FAB) *m*/*z* 269.1285 ($C_{16}H_{17}N_2O_2$ requires 269.1290).

55: ^{1}H NMR 2.37 (s, 6H), 2.43−2.47 (m, 1H), 2.74−2.75 (m, 1H), 3.24−3.29 (m, 1H), 4.35 and 4.38 (two d, 1H, J = 2.9 Hz), 5.88(s, 1H), 7.50−7.57 (m, 2H), 7.90 and 7.95 (two d, 2H, J = 8.2 Hz), 7.97 (s, 1H), 8.27(s, 1H); ^{13}C NMR 40.1, 44.6, 58.9, 82.6, 122.3, 123.8, 126.6, 127.7, 128.5, 129.0, 129.5, 133.6, 135.6, 139.5, 168.0; IR: 3600−3200, 1691; MS (FAB) *m*/*z* 271 (M^+ + 1), 253, 210, 155, 134, 119, 85, 58; HRMS (FAB) *m*/*z* 271.1443 ($C_{16}H_{19}N_2O_2$ requires 271.1447).

56: ^{1}H NMR 2.27 (s, 6H), 2.62 (t, 2H, J = 6.6 Hz), 3.85 (t, 2H, J = 6.7 Hz), 7.66−7.68 (m, 2H), 8.00−8.03 (m, 2H), 8.29 (s, 2H); ^{13}C NMR ($CDCl_3$) 36.1, 45.4, 56.9, 124.6, 127.9, 128.5, 129.1, 130.0, 135.4, 168.1 (C═O); IR: 1699; MS (FAB) *m*/*z* 269 (M^+ + 1), 155, 119, 85; HRMS (FAB) *m*/*z* 269.1298 ($C_{16}H_{17}N_2O_2$ requires 269.1290).

Conversion of 31 to 57−58. A solution of **31** (99 0 mg, 2.14 mmol)) in 150 mL 1:1 CH_3CN−CH_3OH was irradiated for 5 h. Chromatography (silica gel, 10:1 EtAc−hexane) gave **57** (396 mg, 40%) and **58** (198 mg, 20%).

57: mp 191−193 °C (EtAc−hexane); ^{1}H NMR (d_6-DMSO) 0.00 (s, 9H), 1.88 and 2.17 (two d, 2H, J = 15.5 Hz), 2.09 and 2.12 (two d, 1H, J = 3.5 Hz), 2.56 (s, 3H), 2.70 and 2.72 (two d, 1H, J = 5.0 Hz), 2.83 (s, 3H), 2.96−3.02 (m, 1H), 3.44, 3.46, and 3.49 (three d, 1H, J = 5.15 Hz), 3.58 and 3.61 (two d, 1H, J = 7.2 Hz), 3.71 and 3.72 (two d, 1H, J = 3.5 Hz), 4.18 and 4.21 (two d, 1H, J = 4.5 Hz), 5.1 (s, 1H), 7.61−7.65 (m, 2H), 7.95 and 8.00 (two d, 2H, J = 8 Hz), 8.03 (s, 1H), 8.34 (s, 1H); ^{13}C NMR −0.9, 34.7, 34.8, 41.6, 44.2, 44.9, 46.6, 65.7, 87.1, 122.4, 124.7, 127.5, 128.5, 128.9, 129.9, 130.1, 134.1, 135.3,

138.7, 165.1; IR: 3600−3200, 1659; MS (FAB) *m*/*z* 462 ($M^+ + 1$), 382, 329, 267, 250, 194, 155, 116, 73; HRMS (FAB) *m*/*z* 462.1888 ($C_{22}H_{32}N_3O_4SSi$ requires 462.1883).

58: mp 152−154 °C (EtAc−hexane); ^{1}H NMR 0.15 (s, 9H), 2.14 (d, 2H, $J = 11.5$ Hz), 2.58 (t, 2H, $J = 5.5$ Hz), 2.70 (d, 2H, $J = 4$ Hz), 2.97−3.02 (m, 4H), 3.36−3.51 (m, 4H), 4.20 and 4.22 (two d, 1H, $J = 2.5$ Hz)5.28 (s, 1H),7.49−7.57 (m, 2H), 7.88 and 7.90 (two d, 2H, $J = 8$ Hz), 7.97 (s, 1H), 8.22 (s, 1H); ^{13}C NMR −1.6, 36.2,37.1, 37.7, 46.6, 52.2, 54.1, 62.8, 85.3, 121.4, 123.8, 126.8, 127.8, 128.5, 129.2, 129.4, 133.6, 135.0, 140.3, 164.8; IR: 3600−3200, 1691; MS (FAB) *m*/*z* 462 ($M^+ + 1$), 444, 365, 267, 235, 208; HRMS (FAB) *m*/*z* z 462.1886 ($C_{22}H_{32}N_3O_4SSi$ requires 462.1883).

Conversion of 31 to 59 and 60−61. Two solutions of **31** (0.3 g, 0.65 mmol) in 147 mL of 1:1 CH_3OH-CH_3CN and 3 mL 0.02 M $HClO_4$ were irradiated for 1.5 h. One photolysate was concentrated in vacuo to give a residue which was subjected to column chromatography (silica gel, 10:1 EtAc−hexane) giving **59** (0.16 g, 65%). The other photolysate was treated with Na_2CO_3 and then concentrated in vacuo to give a residue which was subjected to column chromatography (silica gel, 10:1 EtAc−hexane) giving **60** (0.2 g, 78%), and **61** (0.03 g, 10%).

59: mp 224−226 °C (EtAc−hexane); ^{1}H NMR 2.32 (s, 3H), 2.77−2.81 (m, 4H), 3.01 (s, 3H), 3.11−3.61 (m, 2H), 4.36 (s, 2H). 6.12 (s, 1H), 7.54−7.59 (m, 2H), 7.90 and 7.99 (two d, $J = 8$ Hz), 8.09 (s, 1H), 8.35 (s, 1H); ^{13}C NMR 36.6, 41.6, 47.0, 53.2, 58.7, 58.9, 102.3, 119.0, 124.1, 126.5, 127.4, 128.4, 128.9, 130.0, 132.0, 133.8, 135.3, 140.6, 167.7. IR: 3011, 1699; MS (FAB) *m*/*z* 372 ($M^+ + 1$), 292, 249; HRMS (FAB) *m*/*z* 372.1375 ($C_{19}H_{22}N_3O_3S$ requires 372.1382).

60: mp 216−218 °C (EtAc−hexane); ^{1}H NMR 2.51 (s, 3H), 2.72−2.78 (m, 5H), 2.88−2.95 (m, 1H), 3.02−3.04 (m, 1H), 3.59−3.66 (m, 2H), 3.87 (d, 1H, $J = 14$ Hz), 3.98−4.03 (m, 2H), 4.51 (d, 1H, $J = 15.5$ Hz), 7.50−7.57 (m, 2H), 7.87 and 7.94 (two d, 2H, $J = 8$ Hz), 7.89 (s, 1H), 8.27 (s, 1H); ^{13}C NMR 36.8, 39.9, 46.7, 48.8, 56.8, 57.1, 58.2, 87.6, 120.7, 123.9, 126.6, 127.7, 128.3, 129.3, 133.3, 135.1, 141.4, 167.0; IR: 3600−3200, 1699; MS (FAB) *m*/*z* 390 (M + 1), 372, 310, 235; HRMS (FAB) *m*/*z* 372.1373 (M − H_2O, $C_{19}H_{22}N_3O_3S$ requires 372.1382).

61: mp 172−174 °C (EtAc−hexane); ^{1}H NMR 1.94 (s, 3H), 2.43 (s, 3H), 2.53 (d, 1H, $J = 13.1$ Hz), 2.58 (d, 1H, $J = 15.3$ Hz), 2.73−2.81 (m, 5H), 2.95 and 3.00 (two d, 2H, $J = 13.7$ Hz), 3.23 (t, 2H, $J = 13.1$ Hz), 3.84 (d, 1H, $J = 14.4$ Hz), 4.53 and 4.90 (two d, 2H, $J = 14.7$ Hz), 7.51−7.61 (m, 2H), 7.95−8.01 (m, 3H), 8.31 (s,1H); ^{13}C NMR 39.3, 41.3, 43.7, 46.7, 49.6, 49.8, 54.0, 58.8,93.9, 123.6, 123.7, 127.4, 128.4, 128.8, 129.5, 129.8, 133.8, 135.0, 136.7, 168.2. IR: 1695; MS (FAB) *m*/*z* 403 (M + 1)), 324, 324, 242; HRMS (FAB) *m*/*z* 403.1336 ($C_{20}H_{23}N_2O_5S$ requires 403.1328).

Conversion of 32 to 52. A solution of **32** (100 mg, 0.2 mmol) in 150 mL of MeOH was irradiated for 7 h. Column chromatography (silica gel, 1:1 EtOAc−hexane) gave 56 mg (70%) of **52**; mp 178−180 °C; ^{1}H NMR 2.96 (s, 3H), 3.65 (m, 12H), 6.33 (s, 1H), 7.53 (m, 2H), 7.95 (m, 1H), 8.32 (s, 1H), 8.36 (s, 1H); ^{13}C NMR 35.8, 40.9, 50.1, 67.8, 69.7, 69.9, 70.8, 108.1, 123.9, 124.5, 127.0, 127.5, 128.1, 129.5, 133.5, 135.6, 166.5; MS (FAB) *m*/*z* 404 (M + 1)), 372, 324, 249, 119, 73, 58; HRMS (FAB) *m*/*z* 404.1643 ($C_{20}H_{26}N_3O_4S$ requires 404.1644).

Conversion of 33 to 53. A solution of **33** (300 mg, 0.7 mmol) in 150 mL of MeOH was irradiated for 9 h. Column chromatography (silica gel, 2:1 EtOAc−hexane) gave 180 mg (80%) of **53**; mp 278−280 °C; ^{1}H NMR 2.11 (s, 3H), 3.78 (m, 8H), 6.47 (s, 1H), 7.54 (m, 2H), 7.93 (m, 2H), 8.07 (s, 1H), 8.34 (s, 1H); ^{13}C NMR 22.9, 41.1, 50.2, 70.0, 70.8, 106.0, 118.7, 124.3, 126.0, 127.3, 128.4, 128.7, 129.8, 131.6, 133.6, 135.2, 137.0, 172.1, 176.5; MS (FAB) *m*/*z* 323 (M + 1)), 322, 291, 152, 118; HRMS (FAB) *m*/*z* 322.1330 ($C_{219}H_{18}N_2O_3$ requires 322.1317).

Conversion of 34 to 49. A solution of **34** (50 mg, 19 mmol) and tetrabutylammonium hydroxide (19 mL, 1.0 M in MeOH) in 100 mL of MeOH was irradiated for 1 h. Chromatography (silica gel, 10:1 EtAc) gave **49** (90%).

Conversion of 35 to 54 and 56. A solution of **35** (100 mg, 0.32 mmol) and tetrabutylammonium hydroxide (0.32 mL, 1.0 M MeOH) in 200 mL of MeOH was irradiated for 7 h. Column chromatography (silica gel, 10:1 EtOAc−hexane) gave 56 mg (65%) of **54** and 10 mg (12%) of **56**.

Photoreaction Quantum Yield Measurements. The actinometers used for measurements of the quantum yields for disappearance of the phthalimide substrates are the TMS-substituted *N*-methansulfonamide **4** ($\phi = 0.12$)[17] and *N*-methylamine **2** ($\phi = 0.04$).[16] Solutions (ca. 1×10^{-5} M, 5 mL) of the substrates and appropriate actinometer in MeOH, whose concentrations were adjusted to bring about equal absorbances at 293 nm, were simultaneously irradiated with Pyrex glass filtered light in a merry-go-round apparatus. Aliquots of the photolysates were removed periodically over a 5−30 min interval, and their absorbances at 293 nm were determined. The disappearance quantum yields (averages of six independent measurements) were determined by comparing the percent disappearance of the substrate to that of the actinometer for photoreactions run at low conversion (5−30%).

Relative quantum yields for the disappearance of the naphthalimide derivatives were determined by using a procedure similar to that described above. In this case, solutions (ca. 1×10^{-5} M, 5 mL) of the naphthalimide substrates in 1:1 MeCN−MeOH, whose concentrations were adjusted to bring about equal absorbances at 256 nm, were irradiated simultaneously by using Pyrex glass filtered light. The disappearance quantum yields, determined at low conversions (<25%), are recorded in Table 4 relative to that of the naphthalimide **27**, which is given a value of one.

Fluorescence Quantum Yield Measurements. Fluorescence quantum yields of the naphthlimide substrates were determined by using *N*-methyl-2,3-naphthalimide as the actinometer ($\phi_f = 0.30$).[23] Solutions (ca. 1×10^{-5} M) with equal absorbances at 256 nm were employed. The fluorescence quantum yields are determined by comparing the intensities of the emission band at 388 nm for each substrate with that of the actinometer.

Acknowledgment. U.C.Y. acknowledges the financial support provided for this research by the Korea Science and Engineering Foundation through the International Cooperative Research Program 2002-5-123-01-2. P.S.M. acknowledges the financial support for this research program by the National Science Foundation (CHE-0130943 and INT-0121510).

Supporting Information Available: Experimental procedures and ^{1}H and ^{13}C NMR spectra for all previously uncharacterized compounds which were prepared in this study (PDF). This material is available free of charge via the Internet at http://pubs.acs.org.

JA0305712